UNIVERSITY OF HELSINKI

https://helda.helsinki.fi

Iron isotope evidence in ocean island basalts for plume- and plate-controlled melting, São Miguel, Azores

Ruttor, Saskia; Nebel, Oliver; Williams, Helen; Beier, Christoph; Richter, Marianne ...

2022-10-15
Elsevier Ltd.
http://hdl.handle.net/10138/585351
Ruttor, S, Nebel, O, Williams, H, Beier, C, Richter, M, Nebel-Jacobsen, Y, Romer, R H W, Turner, S P & Soderman, C R 2022, 'Iron isotope evidence in ocean island basalts for plume- and plate-controlled melting, São Miguel, Azores', Geochimica et Cosmochimica Acta, vol. 335, pp. 111-123. https://doi.org/10.1016/j.gca.2022.08.018

Downloaded from Helda, University of Helsinki institutional repository. https://helda.helsinki.fi
This is an electronic reprint of the original article.
This reprint may differ from the original in pagination and typographic detail.
Please cite the original version.

Iron isotope evidence in ocean island basalts for plume- and plate-controlled melting, São Miguel, Azores

Saskia Ruttor[1]*, Oliver Nebel[1], Helen Williams[2], Christoph Beier[3], Marianne Richter[1], Yona Nebel-Jacobsen[1], René H.W. Romer[4] and Simon P. Turner[5], Caroline R. Soderman[2]

1 School of Earth, Atmosphere and Environment, Monash University, Melbourne, Australia, saskia.ruttor@monash.edu

2 Department of Earth Sciences, University of Cambridge, Cambridge, CB2 3EQ, UK

3 Department of Geoscience and Geography, University of Helsinki, P.O. Box 64, FIN-00014 Helsinki, Finland

4 GeoZentrum Nordbayern, Friedrich-Alexander-Universität Erlangen-Nürnberg (FAU), Schlossgarten 5, D-91054 Erlangen, Germany

5 Department of Earth and Environmental Sciences, Macquarie University, Australia

Abstract

Primitive ocean island basalts (OIB) display a large variability in stable iron (Fe) isotopes, beyond what can plausibly be explained by partial melting and crystal fractionation processes. This Fe isotopic heterogeneity is widely ascribed to inheritance from various exotic mantle components of enriched crustal origin, i.e., subducted and resurfacing oceanic or continental crust, its underlying lithosphere or overlying sediments. These enriched mantle components are characterised by variations in radiogenic Sr-Nd-Pb-Hf isotopes. The extent to which the inherited Fe isotopic signature of subducted and recycled material influences the Fe isotopic composition of OIB and which role secondary processes accompanied with partial melting play is, however, not well understood. The eastern Azores island of São Miguel displays a systematic change from a mantle source less radiogenic in Sr-Nd-Hf-Pb isotopes in the West to a highly enriched source in the East. These variations are among the largest reported in an OIB, indicating variable source component additions to the melt that offer a natural laboratory to elucidate sub-oceanic island processes. Among these, the eastern São Miguel component is unique amongst global OIB in that it has both, extremely radiogenic $^{206}Pb/^{204}Pb$ and $^{87}Sr/^{86}Sr$ isotopic ratios. The spatial distribution, complexity and uniqueness of these isotopic source characteristics are ideally suited to gain insights into the spatial distribution

of mantle components and their potential controls on Fe isotope systematics. Comparing $\delta^{57}Fe_{prim}$, which is the isotopic composition calculated to primitive lavas along a liquid line of descent, with $^{87}Sr/^{86}Sr$, $^{143}Nd/^{144}Nd$, $^{206}Pb/^{204}Pb$ and $^{208}Pb/^{204}Pb$ reveals that the depleted component of western São Miguel shows a heavy Fe isotopic composition ranging from $\delta^{57}Fe_{prim}$ = +0.09 to +0.18‰ (excluding one outlier at -0.02‰ $\delta^{57}Fe_{prim}$), whereas the enriched component of eastern São Miguel shows lighter $\delta^{57}Fe_{prim}$ = +0.05 to +0.12‰. Both suites show a continuum of isotopic compositions between two apparent endmembers. The light Fe isotopic signature of eastern São Miguel lavas, coupled with elevated Rb/Sr and K_2O, indicate K-rich mantle metasomatism in their source. The Fe isotopic composition of western São Miguel's lavas are likely related to a similar source, but have been overprinted by the active Terceira Rift. The latter adds low-degree mid-ocean ridge basalt (MORB)-type melts to the original OIB, likely in the form of a re-fertilised depleted mantle component that underpins the ultraslow spreading region. The two-component mix that contributes to western São Miguel lavas highlights that both enriched mantle components and shallow crustal features can add to the Fe isotopic signatures of erupting OIB, with spatial separation within single volcanic islands. This suggests that a careful evaluation of local geologic features, such as rifting, is required when OIB are probed for their mantle sources, and that heavy Fe isotopic signatures in OIB may not reflect deep, plume-source lithologies. In summary, São Miguel lavas are sourced by a mantle plume, but within a spatially controlled region accompanied by a plate-controlled melt associated with a rifting zone. This dichotomy adds another complication to the genesis of OIB, which however maybe elucidated through combined radiogenic-stable isotope systematics.

Key words: Fe isotopes, Azores, melting, rift, peridotite, metasomatism

1. Introduction

The subduction and recycling of crustal material over hundreds of millions of years has introduced crustal signatures in an otherwise predominantly depleted upper mantle. These crustal signatures are composed of oceanic or continental crust and their lithospheric mantles, and are best traced through radiogenic Sr-Nd-Pb-Hf isotopic ratios of mantle-derived lavas

(Zindler and Hart, 1986; Hart et al., 1992; Hofmann, 1997; Lassiter and Hauri, 1998; Salters and White, 1998; Stracke, 2012; Hofmann and Farnetani, 2013; Koppers et al., 2021;). OIB away from plate margins record complex patterns of radiogenic Sr-Nd-Pb-Hf isotopes with distinct combinations in individual OIB locations (e.g., Hofmann, 2003; Stracke et al., 2005; White, 2015). Mass balance considerations for these trace elements suggest that these lavas sample isotopically enriched sources as remnants of crustal recycling in conjunction with more primitive mantle plume material (Zindler and Hart, 1986; Lassiter and Hauri, 1998; Stracke, 2012; Pietruszka et al., 2013). Diversity in radiogenic isotopes within single plumes indicate that both, plume sources and processes during ascend create mixing patterns of depleted prevalent mantle (PREMA) and recycled, crustal material termed enriched mantle component 1 and 2 (EM1/2), and HIMU (high $^{238}U/^{204}Pb$; Zindler and Hart 1986). These OIB radiogenic isotopic signatures of so-called mantle components are well documented, yet their complex distribution even within single plume regions (e.g., Hawai'i, Iceland, Azores) indicate petrologic complexities superimposed on simple source component distribution patterns (Kurz et al., 1990; Blichert-Toft and Albarede, 1998; Fitton et al., 2003; Weis et al., 2011). Nature, loci and origin of these petrologic processes including secondary processes in the lithospheric mantle in addition to plume-related primary asthenospheric processes, however, remain elusive.

São Miguel, an island of the Azores in the Atlantic Ocean, displays a wide range of radiogenic isotopic compositions, extending from an isotopically less enriched source at western São Miguel (radiogenic isotopic composition similar to PREMA as well as enriched MORB; see discussion in Beier et al., 2007; Beier et al., 2018) to a source composition unique in combined elevated radiogenic Sr, Nd and Pb isotopic signatures at eastern São Miguel (Beier et al., 2007; Elliott et al., 2007; Turner et al., 2007; Beier et al., 2018). The sources are geographically separated but generally tend to show an increasing degree of enrichment in radiogenic isotopes and trace element compositions from West to East (Turner et al., 1997; Widom et al., 1997; Beier et al., 2007; Elliott et al., 2007). The distribution of geochemical signatures is directly linked to individual fault systems related to the slow spreading Terceira Rift axis (Haase and Beier, 2003). The melting processes and the mantle source(s) that cause eastern São Miguel's unique enriched and western São Miguel's less enriched radiogenic isotopic signature is still under debate (e.g., Kurz et al., 1990; Widom et al., 1997; Haase and

Beier, 2003; Widom and Farquhar, 2003; Beier et al., 2006; Beier et al., 2007; Elliott et al., 2007). A prevalent problem in resolving isotopic heterogeneity in plume sources like the ones feeding São Miguel is elusive, and complex petrogenetic mixing during (i) plume ascent, (ii) partial melting and (iii) potential magma reservoir dynamics (e.g., mush reservoirs) *en route* to the surface may contribute to heterogenous isotopic signatures of erupting lavas.

To understand magmatic processes and mantle material that generate OIB at São Miguel, we use new stable Fe isotopes in conjunction with traditional radiogenic isotopes. Over the past decade, stable Fe isotopes have been established as a tool to identify the lithology of mantle components that generate OIB (Williams and Bizimis, 2014; Konter et al., 2016; Nebel et al., 2019). Furthermore, due to its sensitivity to Fe redox state and associated bonding in crystal lattices or melts (Sossi and O'Neill, 2017), Fe isotopes are a useful tracer for magmatic processes such as partial melting, crystal fractionation and mantle metasomatism (Beard and Johnson, 2004; Williams et al., 2005; Weyer and Ionov, 2007; Poitrasson et al., 2013).

The variance in radiogenic isotopes on a km-scale and the uniqueness of the eastern source composition renders lavas from São Miguel suitable to resolve potential magmatic processes that add to the diversity in radiogenic isotopic signatures in OIB. Our data reveal a heavy Fe isotopic signature for western São Miguel's lavas and a relatively light Fe isotopic composition for eastern São Miguel's lavas. The differences in Fe isotopes between eastern and western São Miguel can be ascribed to a source dependency given the good correlations between stable Fe isotopes and radiogenic Sr, Nd and Pb ratios. Crustal material is generally ascribed to heavier Fe isotopic compositions as analysed for western São Miguel. Several processes, among other low degree mantle metasomatism, will be discussed in the following. The heavy Fe isotopic composition of wester São Miguel's lavas might result from rift-related metasomatism associated with the ultraslow Terceira Rift.

2. Geological setting

The Azores archipelago consists of nine volcanic islands where the islands of São Miguel, Terceira and Graciosa and the submarine seamount João de Castro (Romer et al., 2021; Fig. 1a) are located along the ultraslow spreading Terceira Rift (extension rates of 2 – 4 mm/year; Searle, 1980; Vogt and Jung, 2004). São Miguel consists of four stratovolcanoes, which are from West to East, Sete Cidades, Agua de Pau, Furnas and Nordeste (Fig. 1b). The

western part of São Miguel is dominated by the central volcano Sete Cidades (Beier et al., 2006). To the East of Sete Cidades, the so-called Waist Zone consists of a series of scoria cones (Booth et al., 1978; Fig. 1b). The Sr isotopic signatures of the southern scoria cones imply mixing with a source underneath Sete Cidades, whereas the northern scoria cones display Sr isotopic signatures indicating mixing with the eastern volcano of Agua de Pau (Haase and Beier, 2003). Sete Cidades and the western Waist Zone scoria cones are situated along the NW-SE striking Terceira Rift axis (Fig. 1b). In contrast, the eastern part of São Miguel consists of three central volcanoes Agua de Pau, Furnas (not sampled for this study) and Nordeste, aligned in an EW direction. The eastern volcano of Nordeste is inactive and dated to be ~800 kyrs (Johnson et al., 1998). With the exception of Nordeste, all volcanoes on São Miguel are active (Duncan et al., 2015).

From the western islands (Graciosa, Faial, Pico and São Jorge) of the Azores, located closest to the neighbouring mid-Atlantic Ridge, to the eastern islands (Terceira, São Miguel and Santa Maria), the thickness of lithosphere increases (Beier et al., 2008; Béguelin et al., 2017). São Miguel lavas erupted on lithosphere with ~70-80 km thickness and have been generated from melts that form in the garnet stability field as evident by elevated Middle Rare Earth Elements (REE) relative to the Heavy REE Ytterbium (Yb; Beier et al., 2007).

As part of the Azores, São Miguel is situated above the northern Atlantic Large Low Shear Velocity Province (LLSVP), which could be considered to be an indicator for a deep mantle plume origin, also suggested by tomographic models (King and Adam, 2014). However, a deep origin of the Azores mantle plume is a matter of active debate due to elevated volatile contents (Beier et al., 2012; Métrich et al., 2014) and noble gas isotope data from São Miguel, which are comparable to MORB values (Kurz et al., 1990; Moreira et al., 2012; Moreira et al., 2018).

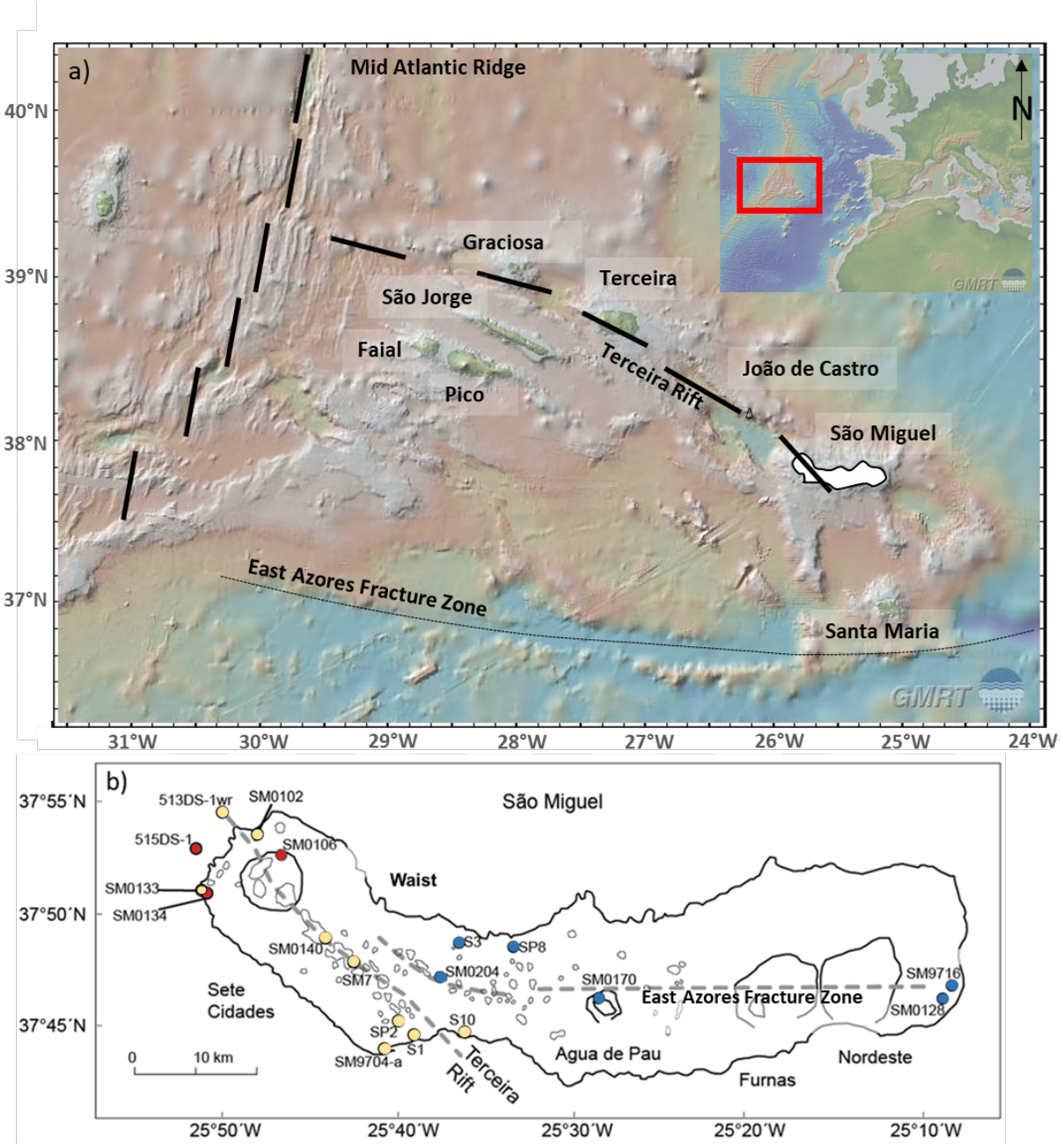


Figure 1. a) The map shows the Azores with João de Castro, Terceira, Graciosa and north-west of São Miguel located on the Terceira Rift. Maps are from the GeoMapApp by Ryan et al. (2009); http://www.geomapapp.org/. b) Map modified after Beier et al. (2007) showing the sample localities. At the volcanic *Waist Zone* (Booth et al., 1978), São Miguel is divided into western (yellow circle) and eastern (blue circle) area, samples in red circles have been excluded from the discussion, because samples have been affected by magnetite fractionation (see 4.1). The main tectonic features are highlighted by grey dotted lines (adopted from Forjaz, 1986), with Sete Cidades being located on the active Terceira Rift and the eastern volcanoes being located parallel to the inactive East Azores Fracture Zone.

3. Sample selection and analytical methods

3.1 Sample selection

We have selected 18 fresh, well-characterised alkali basalts from São Miguel (total alkali silica (TAS) diagram Supplementary Data Fig. S1) and divided them into western (basalts) and eastern (trachybasalts) São Miguel based on their geological features (Forjaz, 1986; Haase and Beier, 2003) and published Sr, Nd and Pb isotopic compositions (Turner et al., 1997; Beier et al., 2007; Elliott et al., 2007; Prytulak et al., 2014). Lavas from western São Miguel include four samples from Sete Cidades and five samples from the southern rift zone of the Waist Zone; eastern São Miguel lavas are those from the northern rift zone of the Waist Zone with three samples, one sample from the Agua de Pau and two samples from Nordeste (Beier et al., 2018; Fig. 1b). The samples SM0133, SM0102, 513DS-1wr, SM0170, SM0128, SM9716, SM0204 have been described by Beier et al. (2006) and Beier et al. (2007) as "*optically fresh and lack of alteration of olivine crystals and vesicle fillings"*. According to Beier et al. (2006) other samples show iddingsitized olivine rims and clay filling in cracks and vesicles. For the whole rock analyses "*fresh cores of these whole rocks were cut, coarse crushed and washed in ionized water and then fine crushed in an agate ball mill"* (Beier et al., 2006; p. 1379). Sample SM07 is described by Elliott et al. (2007) as a basalt that shows olivine and clinopyroxene phenocrysts, and by Prytulak et al. (2014) as a sample that is displaying *"little petrographic or geochemical evidence for contamination*". Turner et al. (1997) described the samples S1, S10, SP2, S3 and SP8, which contain olivine as the main phenocryst phase. A more detailed description of the samples and the Azores chemistry is given in Beier et al. (2007) and Beier et al. (2008) and summarised in Beier et al. (2018) and Larrea et al. (2018). Major and trace element as well as radiogenic isotopic data for all samples analysed in this study are summarised in the Research Data. In brief, the samples are primitive alkali-rich lavas with a range of SiO_2 content from ca. 45-49 wt.%, classifying them as basalts and trachy-basalts, with two samples falling into the basanite field. The lavas contain a classical heavy REE depletion, indicating melting in the presence of garnet and follow a classical liquid line of descent through fractional crystallisation. Radiogenic Sr-Nd isotopes follow a coupled trend similar to other Azores islands, with West São Miguel being more radiogenic in Nd and less radiogenic in Sr compared to East São Miguel.

186 *3.2 Analytical methods*

187 We analysed well characterised samples previously published for their major, trace
188 element and Sr-Nd-Pb isotopic compositions by Turner et al. (1997), Beier et al. (2007), Elliott
189 et al. (2007) and Prytulak et al. (2014) for their stable Fe isotopic compositions. For rock
190 dissolution, ~25 mg of rock powder has been weighed into PFA Teflon beakers and treated
191 with 2 mL concentrated HF:HNO_3 (ratio 1:2). Samples were dissolved for a maximum of three
192 days on a hotplate at 120°C. After evaporation, samples were re-dissolved with small volumes
193 of concentrated nitric acid and a drop of per-oxide to ensure the breakdown of fluoride bonds
194 (Cheng et al., 2014), and finally taken up in 9M HCl (Monash University) or 6M HCl (Durham
195 University) and pipetted onto the AG-MP-1 (Monash University) or AG1-X4 (Durham
196 University) anionic resin (Cheng et al., 2014), which was preconditioned with 9M HCl (Monash
197 University) or 6M HCl (Durham University). Column chromatographic extraction with 9M HCl,
198 6M HCl and 5M HCl removed matrix elements as well as semi and transitional metals. The Fe
199 fraction was eluted with 1M HCl. The collected Fe fraction was placed on a hotplate at 90°C.
200 The dried samples were dissolved and taken up in 2% HNO_3. The detailed chromatographic
201 extraction procedure for Fe purification used at Monash University has been reported by
202 Cheng et al. (2014) and Sossi et al. (2015).

203 The Fe isotope analyses were performed on ThermoFisher™ Scientific Neptune plus
204 multi-collector inductively coupled plasma mass spectrometers (MC-ICP-MS) at the Isotopia
205 Laboratory at the School of Earth, Atmosphere and Environment at Monash University,
206 Australia and Durham University. The samples were introduced via a low flow quartz cyclonic
207 spray chamber and a PFA nebuliser. In medium-resolution mode (Sossi et al., 2015), data were
208 collected in per mil notation relative to the IRMM-014 (Durham University) or IRMM-524a
209 (Monash University) bracketing standards, the latter being isotopically identical to IRMM-014
210 (Craddock and Dauphas, 2010), and with ^{5x}Fe being either ^{56}Fe or ^{57}Fe, respectively:

211 $$\delta^{5x}Fe = \left[\frac{^{5x}Fe/^{54}Fe_{Sample}}{^{5x}Fe/^{54}Fe_{IRMM-524a}} - 1\right] x\ 1000 \quad (1)$$

212 Each sample was analysed two to three times from a single dissolution batch to ensure
213 precision and accuracy, and isotope ratios for each sample represent averaged values (Table
214 1). Each single dissolution batch was mixed with an in-house Ni standard solution to correct
215 for instrumental mass bias effects (Sossi et al., 2015). To ensure reliability and comparability

of our Fe isotope data, the basaltic reference materials BCR2, BHVO1, BIR-1 and $FeCl_3$ were analysed (Table 1). The latter is an in-house standard and coincides with analyses at Cambridge University with $\delta^{56}Fe$ = -0.69 ± 0.03‰ (two-standard deviation 2 S.D.) and $\delta^{57}Fe$ = -1.03 ± 0.05‰ (Soderman et al., 2021). BCR2, BHVO1, BIR-1 are in agreement with previously published analyses (BCR2: $\delta^{56}Fe$ = +0.09 ± 0.01‰ (2S.D.) , $\delta^{57}Fe$ = +0.13 ± 0.02‰ in Craddock and Dauphas (2010) and $\delta^{57}Fe$ = +0.14 ± 0.02‰ in Sossi et al. (2015); BHVO1: $\delta^{56}Fe$ = +0.10 ± 0.01‰, $\delta^{57}Fe$ = +0.16 ± 0.01‰ in Craddock and Dauphas (2010); BIR-1: $\delta^{56}Fe$ = +0.05 ± 0.02‰, $\delta^{57}Fe$ = +0.09 ± 0.02‰ in Craddock and Dauphas (2010)). The reproducibility of the method is ±0.03‰ (2S.D.) in $^{57}Fe/^{54}Fe$ relative to the IRMM-524a external standard based on repeated analyses of standard reference materials. The reproducibility of each sample was calculated as the standard deviation from 2-3 repeated analyses and we always use the larger error (external vs. sample-averaged error). At the end of the analysis a procedural blank was analysed and generally showed values below detection level and is thus negligible.

Ascending mantle melts experience significant olivine and minor pyroxene fractionation, which results in the preferential removal of Fe^{2+} (relative to Fe^{3+}) and also affects the Fe isotopic composition of the melts (Williams et al., 2005; Sossi et al., 2012), driving residual melts toward isotopically heavy values (Teng et al., 2008). Correcting the measured $\delta^{57}Fe$ for crystal fractionation is thus essential to ensure a meaningful comparison between stable and radiogenic isotopic compositions of primary melts from OIB. In order to assess the primary melt compositions, termed $\delta^{57}Fe_{prim}$, we apply an olivine fractionation correction to the measured $\delta^{57}Fe$ isotope values (Sossi et al., 2016). By using a temperature dependent fractionation factor $\Delta^{57}Fe_{Min\text{-}Melt} = -0.4*10^6/T^2$ (further outlined in Sossi et al., 2016) and assuming a starting melt composition with $Fe^{3+}/\sum Fe = 0.15$ (Nebel et al., 2019), we are adding olivine (isotopically light Fe) to our sample lavas until a primary melt composition with magnesium number (Mg#=[(Mg/(Mg+Fe^{2+}) x 100]) = 74 was reached. Considering an exchange coefficient for Fe and Mg between olivine and melt $K_{D_{Ol-Melt}}^{Fe-Mg} \sim 0.3$ (Roeder and Emslie, 1970), the Mg# = 74 is in chemical equilibrium with a primitive mantle (PM) Mg# = 90 (Palme and O'Neill, 2014). The term $\Delta^{57}Fe_{Min\text{-}Melt}$ describes the difference between the melt $\delta^{57}Fe_{Melt}$ value and the mineral $\delta^{57}Fe_{Min}$ isotope value (i.e., olivine):

$$\Delta^{57}Fe = \delta^{57}Fe_{Min} - \delta^{57}Fe_{Melt} \quad (2)$$

The starting melt composition with $Fe^{3+}/\sum Fe = 0.15$ is higher than global MORB values of $Fe^{3+}/\sum Fe = +0.12 \pm 0.02$ (Bézos and Humler, 2005) and used for primary melt stable Fe isotope calculations in OIB (Nebel et al., 2019; Soderman et al., 2021) and back-arc basalts (Nebel et al., 2018). OIB glasses from São Miguel have not been analysed for their redox-state rendering this approach a best-estimate.

The main uncertainties of the fractionation correction model lie in the variability of the initial mantle source composition at Mg# = 90 and the fractionation factor between mineral species applied. Pyroxenitic sources can vary from this value (Herzberg, 2011). However, even though the São Miguel mantle source may be heterogeneous, i.e., peridotite and pyroxenite lithologies may variably contribute to the melting regime, a difference of, e.g., Mg# ± 2, results only in $\delta^{57}Fe_{prim} \pm 0.01$‰, which is negligible for the approach applied here (Nebel et al., 2019). A variation of 0.1 unit in the inter-mineral correction factor (e.g., $-0.4*10^6/T^2$ or $-0.3*10^6/T^2$) equates to $\delta^{57}Fe_{prim}$ 0.03‰ variations. Note, smaller correction factors are leading to apparently less pronounced corrections. It needs to be stated here that our applied fractionation factor of $-0.4*10^6/T^2$ is a large extent of correction for basalts ranging from 4.0 – 14.3 wt.% MgO (Soderman et al., 2021). A test for the magnitude of the applied correction using $\Delta^{57}Fe_{Min\text{-}Melt} = -0.4*10^6/T^2$, is further illustrated in Fig. 3, where we compare $\delta^{57}Fe_{prim\text{-}0.1}$ corrected with a $\Delta^{57}Fe_{Min\text{-}Melt} = -0.1*10^6/T^2$. Throughout the manuscript, $\delta^{57}Fe_{prim}$ is shown with a correction factor of $\Delta^{57}Fe_{Min\text{-}Melt} = -0.4*10^6/T^2$, because we will compare our data with other Azores islands (São Jorge, Pico, Faial, Terceira, João de Castro and Graciosa) from Soderman et al. (2021), who used a fractionation factors of $-0.4*10^6/T^2$.

The São Miguel whole rock Fe isotope values are presented both as measured $\delta^{57}Fe$ and as calculated primary melt $\delta^{57}Fe_{prim}$. Errors for $\delta^{57}Fe$ and $\delta^{57}Fe_{prim}$ are reported as the standard deviation of repeated analyses of each sample aliquot from the IRMM-524a (Monash University) or IRMM-014 (Durham University) Fe standards (or ±0.03‰ in case this value is lower). The $\delta^{57}Fe_{prim}$ do not include error propagations of the correction method.

4. Results

4.1 Filtering for wall rock assimilation and magnetite fractionation

We scanned our new data for potential secondary effects by excluding: (1) Samples exceeding a Ba/Rb value of 12 ± 2 (Hofmann and White, 1983), indicative for country rock

assimilation. Exceptions are samples SM9704A and SM0140 with a Ba/Rb of 15.9 and 22.7, respectively, due to their high MgO content of 12.67 and 9.81 wt.%, which precludes assimilation of quartz syenite country rock; (2) Samples with MgO < 4.0 wt.% and TiO_2 < 2.5 wt.% (Fig. 2) due to the influence of magnetite fractionation on the Fe isotopic composition of the remaining melt by preferentially removing isotopically heavy Fe (Sossi et al., 2012, Nebel et al., 2015; Nebel et al., 2019); a feature that cannot adequately be corrected for. For the latter, the excluded samples (SM0106, SM0134, 515DS-1) show high $\Delta^{57}Fe$ (= $\delta^{57}Fe$ – $\delta^{57}Fe_{prim}$) of 0.14 to 0.26‰ (Fig. 3) and are not discussed in detail. Two samples of eastern São Miguel with a MgO content < 5.0 wt.% plot arguably close to the threshold defined by Sossi et al. (2012) and Nebel et al. (2019). These samples, however, show a $\Delta^{57}Fe$ of 0.10 and 0.12‰ with relatively low Ni contents of 18 and 21 ppm (Research Data), and are interpreted as not being affected by the fractionation of magnetite.

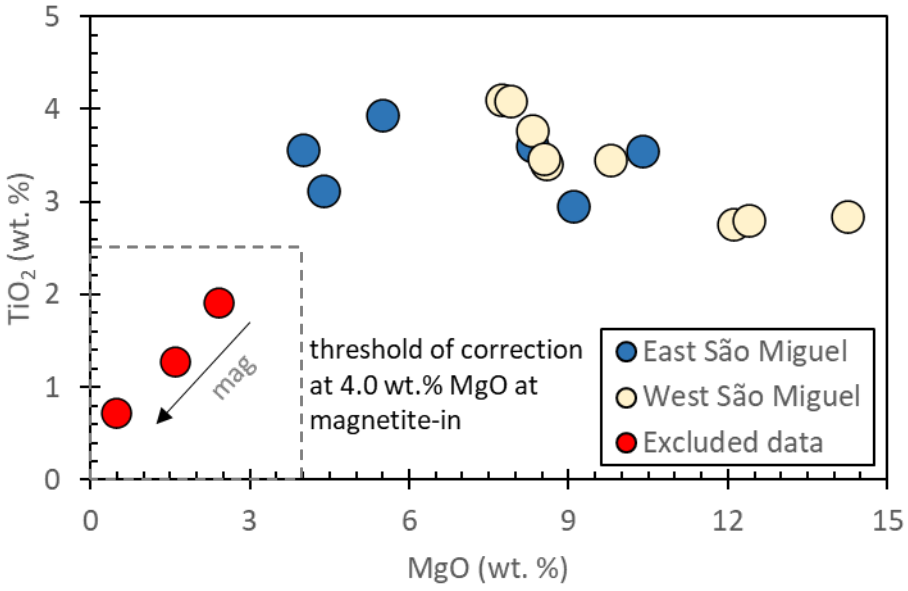


Figure 2. MgO vs TiO_2 contents to illustrate potential magnetite saturation of samples. Our threshold at 4.0 wt.% MgO ensures the exclusion of samples affected by magnetite fractionation. Several studies, e.g., Sossi et al. (2012) and Nebel et al. (2015) show that at low MgO values magnetite is the primary host of Fe. Red circles highlight the samples that have been excluded from the discussion.

4.2 Stable Fe isotopes

Samples from São Miguel have measured $\delta^{57}Fe$ signatures comparable to or heavier than mean MORB ($\delta^{57}Fe$ = +0.15 ± 0.01‰ (2S.D.); Teng et al., 2013; Chen et al., 2019) with a single

297 outlier at western São Miguel (SM0133) which has a lighter Fe isotopic composition than
298 MORB with $\delta^{57}Fe$ = +0.03‰. Generally, $\delta^{57}Fe$ values range from +0.09 to +0.24‰ for eastern
299 São Miguel and from +0.13 to +0.22‰ for western São Miguel lavas, if SM0133 is excluded.

300 The primary magma shows a value of ~12.0 wt.% MgO for lavas from São Miguel. We
301 therefore correct lavas <12.0 wt.% MgO for olivine fractionation. SM0140 with 12.41 wt.%
302 MgO can be left uncorrected. SM0102 with 14.26 wt.% shows presumably olivine
303 accumulation rather than fractionation. Olivine accumulation can only be corrected for when
304 olivine is in equilibrium with the final bulk composition (McCoy-West et al., 2018), which is
305 unlikely in this case. Due to the lack of a statistical difference between high and low MgO
306 lavas, we include SM0102 in the following. After correction for olivine crystal fractionation
307 ($\Delta^{57}Fe_{Min\text{-}Melt} = -0.4*10^6/T^2$), the following, slightly lighter melt $\delta^{57}Fe_{prim}$ compositions are
308 obtained for eastern and western São Miguel lavas: $\delta^{57}Fe_{prim}$ +0.05 to +0.12‰ and +0.09 to
309 +0.18‰ (excluding outlier SM0170 at -0.2‰), respectively. Samples from western São Miguel
310 display the lowest values in both $\delta^{57}Fe$ and $\delta^{57}Fe_{prim}$ (Fig. 3a and b). The crystal fractionation
311 correction factor ($\Delta^{57}Fe$) is largest for eastern São Miguel ranging from $\Delta^{57}Fe$ = 0.04 to 0.12‰,
312 whereas western São Miguel shows lower values with $\Delta^{57}Fe$ = 0.00 to 0.07‰. We note here
313 that this correction is only an approximation of the exact likely liquid line of descent and thus
314 should be treated as such. Nonetheless, even though the effect is minor (Fig. 3b), it better
315 approaches the true nature of primitive melts prior to crystal fractionation.

316

317

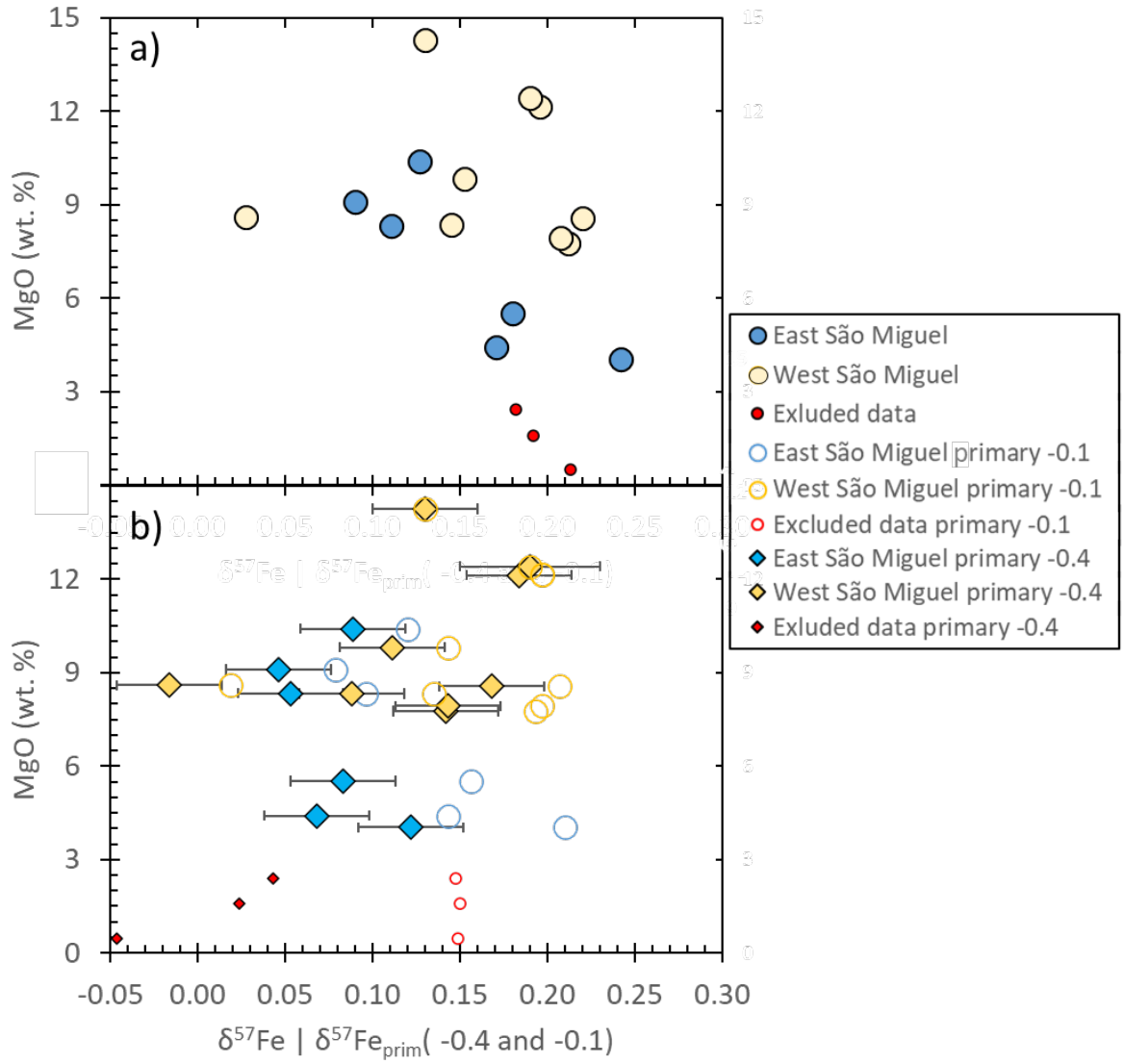


Figure 3. a) Analysed $\delta^{57}Fe$ compositions of eastern and western São Miguel lavas and b) calculated primary melt values $\delta^{57}Fe_{prim}$ (calculated with a fractionation factor of $\Delta^{57}Fe_{ol\text{-}melt} = -0.1*10^6/T^2$, illustrated as empty circles) and $\delta^{57}Fe_{prim}$ (calculated with a fractionation factor of $\Delta^{57}Fe_{ol\text{-}melt} = -0.4*10^6/T^2$, illustrated as diamonds) vs MgO. Crystal fractionation correction after Sossi et al. (2016) and Nebel et al. (2019). Values of error bars shown with ±2 S.E. Error bars just shown for measured $\delta^{57}Fe$ to retain overview. Analysed $\delta^{57}Fe$ of eastern São Miguel samples co-variate with MgO with a mean squared weighted deviation (MSWD) of 1.19.

Table 1. Iron isotope values for São Miguel lavas. Samples with "*" have been analysed at the Durham University. 2 standard error calculated as follows: 2 S.E. = 2 S.D. / $\sqrt{n}$, with *n* being

the number of analyses, after Sossi et al. (2015). Each sample has been analysed 2-3 times (n=2-3). $\Delta^{57}Fe_{prim}$ calculated with $\Delta^{57}Fe_{ol\text{-}melt} = -0.4*10^6/T^2$. For major, trace and radiogenic isotope values see Research Data.

Sample	Location	MgO (wt.%)	$\delta^{56}Fe$	±2 S.E.	$\delta^{57}Fe$	±2 S.E.	$\delta^{57}Fe_{prim}$	$\Delta^{57}Fe$	n
SM0140	Sete Cidades	12.41	+0.13	0.02	+0.19	0.04	+0.19	0	2
SM0133	Sete Cidades	8.60	+0.03	0.01	+0.03	0.03	-0.02	0.04	3
SM0102	Sete Cidades	14.26	+0.07	0.03	+0.13	0.01	+0.13	0	3
513DS-1 wr	Sete Cidades	12.13	+0.14	0.01	+0.20	0.02	+0.18	0.01	3
SM9704A	Waist Zone	9.81	+0.04	0.01	+0.15	0.01	+0.11	0.04	2
S1*	Waist Zone	7.76	+0.12	0.02	+0.21	0.03	+0.14	0.07	3
SM7	Waist Zone	8.56	+0.15	0.03	+0.22	0.02	+0.17	0.05	3
S10*	Waist Zone	8.33	+0.10	0.02	+0.15	0.03	+0.09	0.05	2
SP2*	Waist Zone	7.93	+0.13	0.01	+0.21	0.02	+0.14	0.06	2
SM0170	Agua de Pau	4.41	+0.13	0.02	+0.17	0.02	+0.07	0.10	3
SM0128	Nordeste	4.03	+0.16	0.01	+0.24	0.01	+0.12	0.12	3
SM9716	Nordeste	5.52	+0.11	0.01	+0.18	0.01	+0.08	0.10	3
SM0204	Waist Zone	10.41	+0.10	0.01	+0.13	0.02	+0.09	0.04	3
S3*	Waist Zone	8.34	+0.13	0.00	+0.11	0.03	+0.05	0.06	2
SP8*	Waist Zone	9.10	+0.06	0.02	+0.09	0.03	+0.05	0.04	2
Excluded data									
SM0106	Sete Cidades	0.48	+0.15	0.01	+0.21	0.02	-0.05	0.26	3
SM0134	Sete Cidades	2.41	+0.14	0.01	+0.18	0.01	+0.04	0.14	3
515DS-1	Submarine W Sete Cidades	1.58	+0.15	0.01	+0.19	0.02	+0.02	0.17	3
BCR2			+0.09	0.01	+0.12	0.01			3
BHVO1			+0.09	0.03	+0.11	0.02			2
BIR-1*			+0.06	0.01	+0.08	0.01			2
$FeCl_3$*			-0.69	0.01	-1.03	0.01			25

5. Discussion

Various factors such as fractionation during partial melting and crystallisation (Teng et al., 2008; Williams et al. 2009; Teng et al., 2013), source mineralogy (Weyer and Ionov, 2007; Dauphas et al., 2009; Craddock et al., 2013; Williams and Bizimis, 2014), source inheritance (Konter et al., 2016; Nebel et al., 2019), mixing process of source lithologies (Nebel et al., 2019) and metasomatism or diffusion (Teng et al., 2011; Sun et al., 2020) influence Fe isotopic compositions of OIB. In the following, we will compare $\delta^{57}Fe_{prim}$ with radiogenic isotopic data, major elements and trace elements to evaluate if (5.1) mantle source and mixing processes, (5.2) source mineralogy and melting degree, (5.3) metasomatism and/or (5.4) tectonic setting (e.g., mixing of rift related melt with plume-related mantle material) can explain the Fe isotopic signature of western and eastern São Miguel lavas.

5.1 Source dependency of the Fe isotopic signature of primary melts for eastern and western São Miguel

To evaluate the geochemical source dependency of stable Fe isotopes and to elucidate if potential melt mixing processes are causing the variation in radiogenic isotopic systems and stable Fe isotopic signatures, we compare published $^{208}Pb/^{204}Pb$, $^{206}Pb/^{204}Pb$, $^{87}Sr/^{86}Sr$, $^{143}Nd/^{144}Nd$ values (Turner et al., 1997; Beier et al., 2007; Prytulak et al., 2014) with our new $\delta^{57}Fe_{prim}$ data from western and eastern São Miguel (Fig. 4). Western and eastern São Miguel lavas exhibit very different radiogenic isotopic systematics, and our Fe isotope data needs to be placed into this complex context:

The unique radiogenic isotopic signature of eastern São Miguel is characterised by radiogenic Pb and radiogenic Sr and Nd isotopic compositions. To explain the deviation of eastern São Miguel from commonly observed OIB sources in radiogenic isotopic systems, various mantle sources have been proposed over the last decades (Davies et al., 1989; Beier et al., 2007; Elliott et al., 2007; Moreira et al., 2018). Davies et al. (1989), Turner et al. (1997), Widom and Farquhar (2003), Beier et al. (2007), and Genske et al. (2013) have based their models on mantle source components created from ancient recycled oceanic crust based on oxygen isotopic ($\delta^{18}O$) combined with radiogenic Sr-Nd-Pb isotopic systematics. Furthermore, thick lithospheric roots (infused by metasomatism) or ancient recycled oceanic lithosphere (variably influenced by metasomatism and/or distinct mantle sources) have been suggested for causing the enrichment in radiogenic isotopes (Widom and Farquhar, 2003; Beier et al., 2007; Elliott et al., 2007; Turner et al., 2007). On the basis of radiogenic isotopic compositions

and eastern São Miguel's low helium (^{3}He) signature (R/Ra of 0.4-5.55, lower than MORB with R/Ra 8 ± 1; Moreira et al., 2012), it has been suggested that the source of eastern São Miguel is comprised of ancient, recycled material, subducted at ca. 3 Ga (Elliott et al., 2007). Contrary to eastern São Miguel, western São Miguel lavas show a less radiogenic isotopic signature in $^{208}Pb/^{204}Pb$, $^{206}Pb/^{204}Pb$, $^{87}Sr/^{86}Sr$ and $^{143}Nd/^{144}Nd$ (Fig. 4), which has been proposed to represent a common Azores source component (e.g., Beier et al., 2007; Beier et al., 2018). Additionally, He isotopic signatures of western São Miguel are comparable to MORB (e.g., Kurz et al., 1990).

When combining radiogenic Sr-Nd-Pb isotopic ratios with stable Fe isotopes, lavas from São Miguel show a positive covariation between $^{143}Nd/^{144}Nd$ and $\delta^{57}Fe_{prim}$ and negative trends between $^{208}Pb/^{204}Pb$, $^{206}Pb/^{204}Pb$ and $^{87}Sr/^{86}Sr$ vs. $\delta^{57}Fe_{prim}$ (Fig. 4c-f). These trends between radiogenic isotopes and stable isotopic compositions demonstrate that Fe isotope systematics of São Miguel's lavas are dominated by mantle source variations. "Inherited Fe isotopic compositions from crustal precursors" have been proposed for MORB as well as other OIB (Konter et al., 2016; Nebel et al., 2019; Sun et al., 2020). It is thus plausible, especially considering that trace element ratios and radiogenic isotopic ratios are source dependent (White et al., 1979; Turner et al., 1997; Widom et al., 1997; Beier et al., 2007; Elliott et al., 2007) that São Miguel's Fe isotopic variations, at least to a large degree, reflect an inherited Fe isotopic signature from the source as well. As expected, the one outlier, sample SM0133 with $\delta^{57}Fe_{prim}$ -0.02‰, deviates from the correlation, yet shows radiogenic isotopic values in line with the rest of western São Miguel lavas. The outlier will be discussed further in section 5.4.

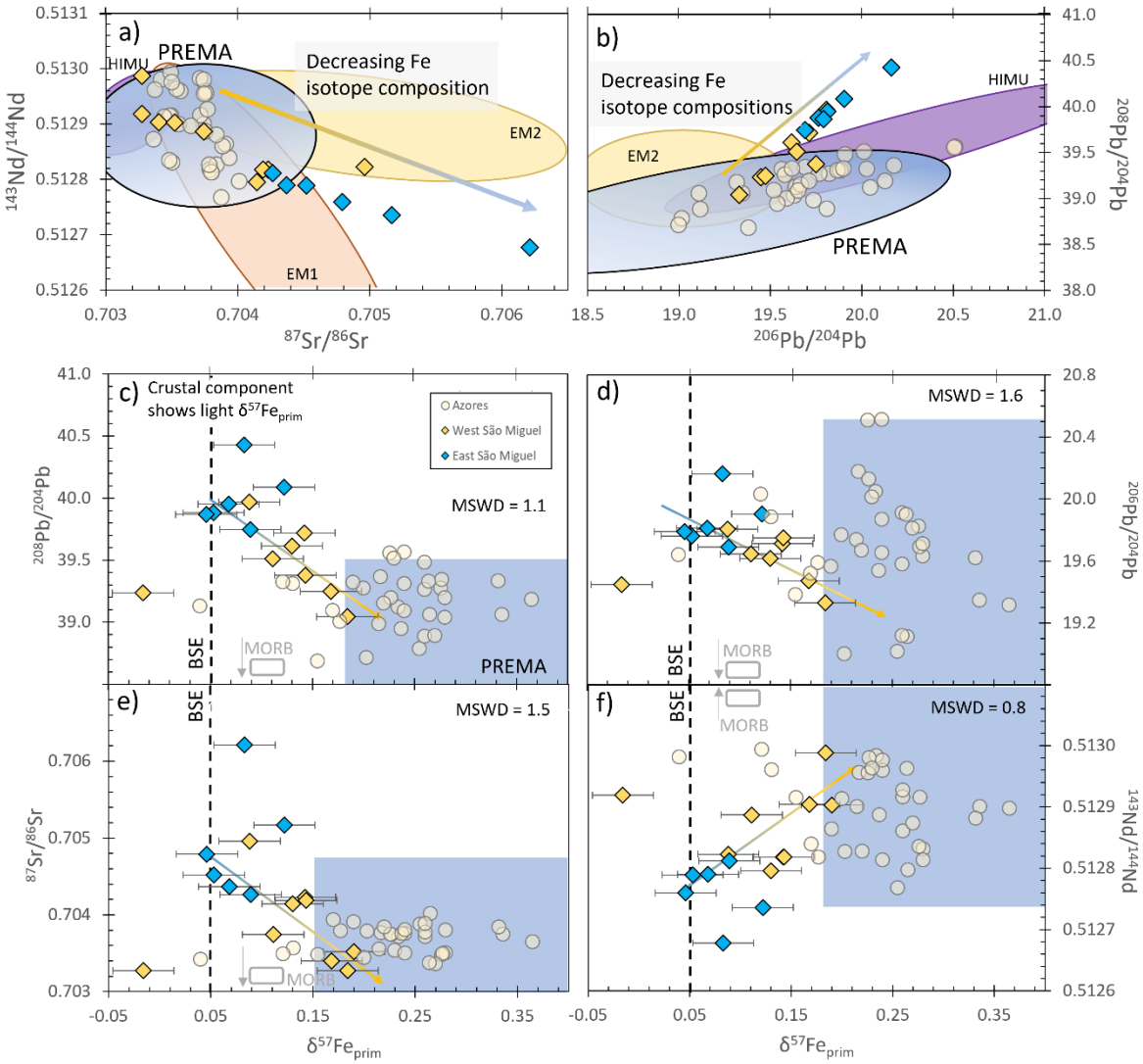


Figure 4. a) $^{87}Sr/^{86}Sr$ vs $^{143}Nd/^{144}Nd$, b) $^{206}Pb/^{204}Pb$ vs $^{208}Pb/^{204}Pb$, and $\delta^{57}Fe_{prim}$ vs c) $^{208}Pb/^{204}Pb$, d) $^{206}Pb/^{204}Pb$, e) $^{87}Sr/^{86}Sr$, f) $^{143}Nd/^{144}Nd$ for eastern and western São Miguel. PREMA area after Stracke et al. (2005), Jackson et al. (2007) and White (2015). MORB +0.10 ± 0.01‰ $\delta^{57}Fe_{prim}$ and bulk silicate earth (BSE) +0.05 ± 0.01‰ $\delta^{57}Fe$ are from Sossi et al. (2016). Azores (São Jorge, Pico, Faial, Terceira, João de Castro and Graciosa) are from Soderman et al. (2021). MSWD calculated after Wendt and Carl (1991). Please refer to text for explanation of mantle components EM1, EM2, HIMU and PREMA.

Enriched radiogenic isotopic signatures in OIB (e.g., EM1) are commonly associated with recycled crustal material, which can be accompanied by small amounts of sediment (Chase, 1981; Hofmann and White, 1982; Stracke, 2012). In the mantle, this recycled crustal material is present as eclogite, presumably interacting with the ambient peridotite to form pyroxenite (Sobolev et al., 2007), which can be heavy in Fe isotopes (Konter et al., 2016; Nebel et al.,

2019; Soderman et al., 2021). However, eastern São Miguel's lavas, which can be associated with recycled crustal material due to the enriched radiogenic isotopic signature, show lighter $\delta^{57}Fe_{prim}$ values than western São Miguel ranging from +0.05 to +0.12‰. Western São Miguel lavas with a less enriched radiogenic isotopic signature show heavier $\delta^{57}Fe_{prim}$ values of up to +0.18‰.

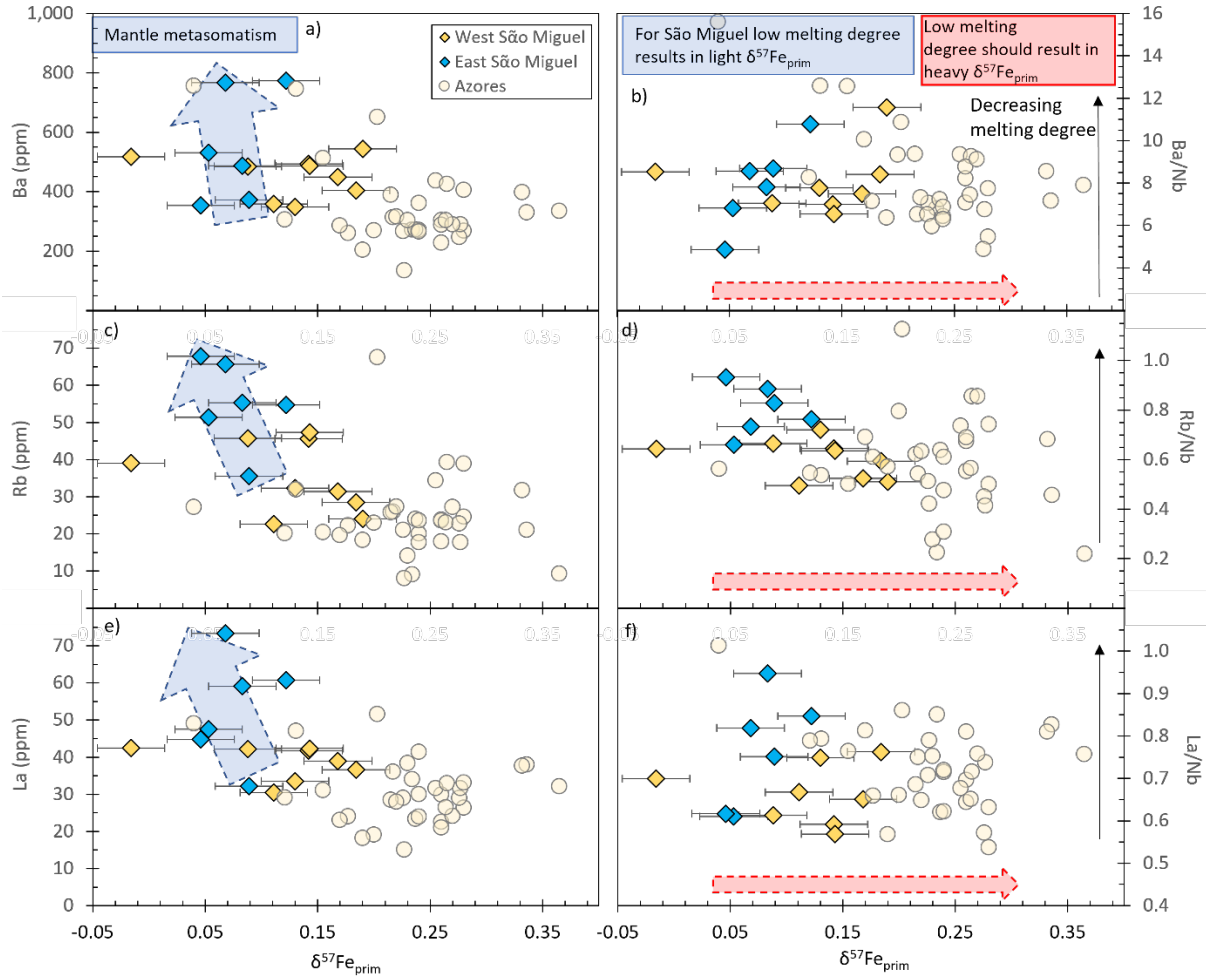
Importantly, in all cases, the assigned trends of the combined stable Fe isotopes and radiogenic Sr-Nd-Pb isotopic ratios of eastern and western São Miguel are surprising. One would expect the more enriched radiogenic isotopic signatures to be associated with heavy $\delta^{57}Fe_{prim}$, if the latter is considered to represent a recycled crustal component (Konter et al., 2016; Nebel et al., 2019) or pyroxenite formed from recycled crustal protoliths (Williams and Bizimis, 2014). The less enriched radiogenic Sr-Nd-Pb isotopic component of western São Miguel coincides with samples from other Azores islands and shows a slightly heavier Fe isotopic signature than eastern São Miguel (Fig. 4a-f). If this 'less enriched isotopic signature' is indeed related to a peridotite source, as opposed to eclogite/pyroxenite, it is in contradiction to the widely accepted view that the isotopically less enriched mantle, which is represented by peridotite (e.g., Zindler and Hart, 1986; Salters and Stracke, 2004), is associated with an Fe isotopic composition of $\delta^{57}Fe = +0.05 \pm 0.01$‰ (2S.E.; Sossi et al., 2016).

5.2 Light Fe isotopes of eastern São Miguel – degree of melting

Isotope fractionation during partial mantle melting, and subsequent crystal fractionation can account for a small variation in Fe isotopes (Teng et al., 2008; Williams et al., 2009; Teng et al., 2013). During partial melting, the crystal bonding dependent partitioning of Fe between liquid and crystalline residue, with ferric iron (Fe^{3+}) being more incompatible than ferrous iron (Fe^{2+}) (Woodland and Koch, 2003), leads to a heavy Fe isotopic signature in the melt. With larger degrees of melting, more olivine enters the melt phase, which leads to a relatively lighter Fe isotopic composition compared to melts that experienced low melting degrees (Williams and Bizimis, 2014).

Beier et al. (2007) and Elliott et al. (2007) compared major elements and trace element ratios to show that Azores islands of São Jorge, Pico, Faial, Terceira, João de Castro and Graciosa have melting degrees (F) ranging between 4 and 6% (Beier et al., 2013), and are subtly larger than those suggested for São Miguel. Subsequently, Beier et al. (2013) showed

that the melting degree of São Miguel lavas on average is similar to that of Santa Maria, an Azores island southeast of São Miguel, with an estimation of ca. F = 2 – 3%. The changes in degree of partial melting may be associated with changes in lithospheric thickness from west to east of the Azores archipelago (Prytulak and Elliott, 2007; Standish et al., 2008). Although there are no apparent differences in melting degrees between and within eastern and western São Miguel (Beier et al., 2013), source compositional variability may be affecting calculations on subtle differences in degrees of melting. Nonetheless, the decoupling of REE, major element systematics and $\delta^{57}Fe_{prim}$ (e.g., $\delta^{57}Fe_{prim}$ vs $(Sm/Yb)_{PM}$ and Ti_8 (TiO_2 content at 8 wt.% MgO); see Supplementary Data Fig. S2) indicates that the variation in Fe isotopes *between* eastern and western São Miguel is not a function of the degree of partial melting in the São Miguel mantle source. It is, however, intriguing that the low melting degree of eastern and western São Miguel are associated with lighter Fe isotopic compositions compared to the Azores islands of São Jorge, Pico, Faial, Terceira, João de Castro and Graciosa (Fig. 5). This is the opposite of what is expected at low degree melting, i.e., enrichment in incompatible elements *and* heavier Fe isotopes. Melting at higher melt degrees results for the Azores lavas in low Ba/Nb, Rb/Nb and La/Nb at heavier $\delta^{57}Fe_{prim}$, whereas western São Miguel lavas show lighter $\delta^{57}Fe_{prim}$ at similar trace element ratios. Eastern São Miguel lavas, showing the lightest $\delta^{57}Fe_{prim}$, deviate towards elevated Rb/Nb and La/Nb ratios. Such enrichment in incompatible elements, here pronounced deviation of eastern São Miguel in $\delta^{57}Fe_{prim}$ vs Rb and La (Fig. 5c, e), combined with light $\delta^{57}Fe_{prim}$ suggests that the otherwise enriched component of eastern São Miguel might have experienced fractionation processes other than crystal fractionation, that lead to a light Fe isotopic signature (e.g., mantle metasomatism in Fig. 5).



455

456 **Figure 5**. a) Ba, b) Ba/Nb, c) Rb, d) Rb/Nd, e) La, f) La/Nb vs $\delta^{57}Fe_{prim}$. Azores (São Jorge, Pico,
457 Faial, Terceira, João de Castro and Graciosa) are from Soderman et al. (2021). Blue arrow
458 shows effect of mantle metasomatism resulting in elevated Ba, Rb and La. Red arrow
459 indicated that low melting degrees should result in heavy Fe isotopic compositions in OIB.

460 *5.3 Light Fe isotopes of eastern São Miguel – mantle metasomatism*

461 To characterise melts and fluids that can act as metasomatising agents in the mantle, it
462 is crucial to understand the Fe isotopic composition of metasomatising agents and how such
463 material alters the inherited Fe isotopic composition of upwelling mantle material.
464 Considering the subduction of MORB and a small input of continental sediments, which show
465 a wide range with δ^{57}Fe +0.08 to +0.90‰ (Du et al., 2017) or arc system sediments with δ^{57}Fe
466 +0.17‰ (Nebel et al., 2015) and loss of light Fe isotopes during hydrothermal alteration (El
467 Korh et al., 2017), most subducted recycled slab components are expected to show a heavy
468 Fe isotopic signature of δ^{57}Fe > +0.15‰. However, in a model in which enriched mantle

components (where enriched refers to radiogenic isotopes) are derived from subducted oceanic crust and/or lithosphere and sediments, a subduction component must exist that is also isotopically light and not heavy in Fe isotopes. Light Fe isotope values have been associated with metasomatising agents such as slab derived melts, subducted sediments, CO_2-rich fluids or carbonatitic melts (Rouxel et al., 2003; Beard and Johnson, 2004; Williams et al., 2005; Weyer and Ionov, 2007; Johnson et al., 2010; Zhao et al., 2012; Poitrasson et al., 2013).

Mantle metasomatism involving such metasomatising agents has been described at several OIB locations, for example, Hawai'i, Pitcairn, Samoa, Kerguelen Island, and the Island of Santa Maria as part of the Azores (Hauri et al., 1993; Mattielli et al., 1999; Sobolev et al., 2000; Weyer and Ionov, 2007; Beier et al., 2013; Poitrasson et al., 2013; Wang et al., 2018). Based on element ratios of Ti/Sm and K/La, Beier et al. (2013) show that mixing of carbonated peridotite with melts from a volatile free garnet peridotite (ratio 20:80) can explain the geochemical composition of Santa Maria. However, a carbonatite melt-mantle mixing model (Supplementary Data Fig. S3) and mass balance calculations using radiogenic Sr-Nd isotopes limit any such addition to no more than 1%. With such a low contribution, a carbonatitic melt must be unrealistically isotopically heavy in Fe to achieve the average Fe isotopic composition of eastern São Miguel's lavas: Considering mass balance calculations, 1% of a carbonatitic component cannot explain the Fe isotopic composition of eastern São Miguel's lavas: assuming that a carbonatite and anhydrous peridotite melt show equal proportions of Fe and considering a contribution of 1% carbonatitic component with $\delta^{57}Fe_{carbonatite}$ = -0.45‰ to a peridotite with $\delta^{57}Fe_{prim}$ = +0.05‰, by mass balance, a $\delta^{57}Fe_{prim}$ of ~ +0.05‰ (min. $\delta^{57}Fe_{prim}$ of eastern São Miguel lavas) can be achieved. The value of $\delta^{57}Fe_{carbonatite}$ = -0.45‰ is a reasonable estimation of carbonatite magmas that are in equilibrium with silicate melts (Johnson et al., 2010). However, to achieve the average $\delta^{57}Fe_{prim}$ of ~ +0.08‰ of eastern São Miguel's lavas, a mixture of peridotite with $\delta^{57}Fe_{prim}$ = +0.05‰ and $\delta^{57}Fe_{carbonatite}$ = +3.0‰ (ratio 99:1) is needed. Such heavy Fe isotopic compositions have not been analysed in carbonatites (Johnson et al., 2010). Irrespective of the true proportions and endmember compositions, considering simplified mass balance calculations, it is apparent that 1% of a carbonatitic component shows either no change between the Fe isotopic composition of the source and the melt or must be unrealistically heavy to achieve the average Fe isotopic

composition of eastern São Miguel's lavas. Increasing the mixing ratio to 80:20 will result in $\delta^{57}Fe_{prim}$ < +0.05‰ and, additionally, contradicts our calculated carbonatite melt-mantle mixing model (Supplementary Data Fig. S3). Thus, we exclude the possibility of a carbonatitic melt as a metasomatising agent for eastern São Miguel's lavas.

A characteristic that might indicate mantle metasomatism is the enrichment in K_2O and Rb/Sr of eastern São Miguel compared to western São Miguel and other Azores islands (Fig. 6). This enrichment indicates the contribution of a potassium(K)-rich mineral, possibly amphibole, phlogopite or a high-pressure phase, such as K-hollandite (LaTourrette et al., 1995). Phlogopite is a mineral commonly associated with mantle metasomatism (Zhao et al., 2012; Safonov et al., 2019) showing heavy $\delta^{57}Fe$ +0.32 to +0.49‰ (Zhao et al., 2012). An interaction of a high-K phase with the melt sourcing eastern São Miguel is thus expected to result in heavy Fe isotope values. With the enrichment in K and Rb/Sr, $^{87}Sr/^{86}Sr$ is increasing (Fig. 6b, d) as a consequence of the high time-integrated parent-daughter ratio. However, $\delta^{57}Fe_{prim}$ is decreasing (Fig. 6a, c), opposite of what is expected if any high-K phase is isotopically heavy in Fe. Solutions to this conundrum could be that (1) the Fe isotopic composition of mantle phlogopite is variable and isotopically light underneath São Miguel, similar to biotite reported elsewhere (Ye et al., 2020); alternatively (2) phlogopite is controlling co-variation of Sr, Nd and Pb isotopes with K_2O and Rb/Sr (Fig. 6, Supplementary Data Fig. S4), yet with a negligible Fe content, whereas isotopically light Fe is added by a separate phase that is rich in Fe so that both processes – phlogopite + unknown phase are additive.

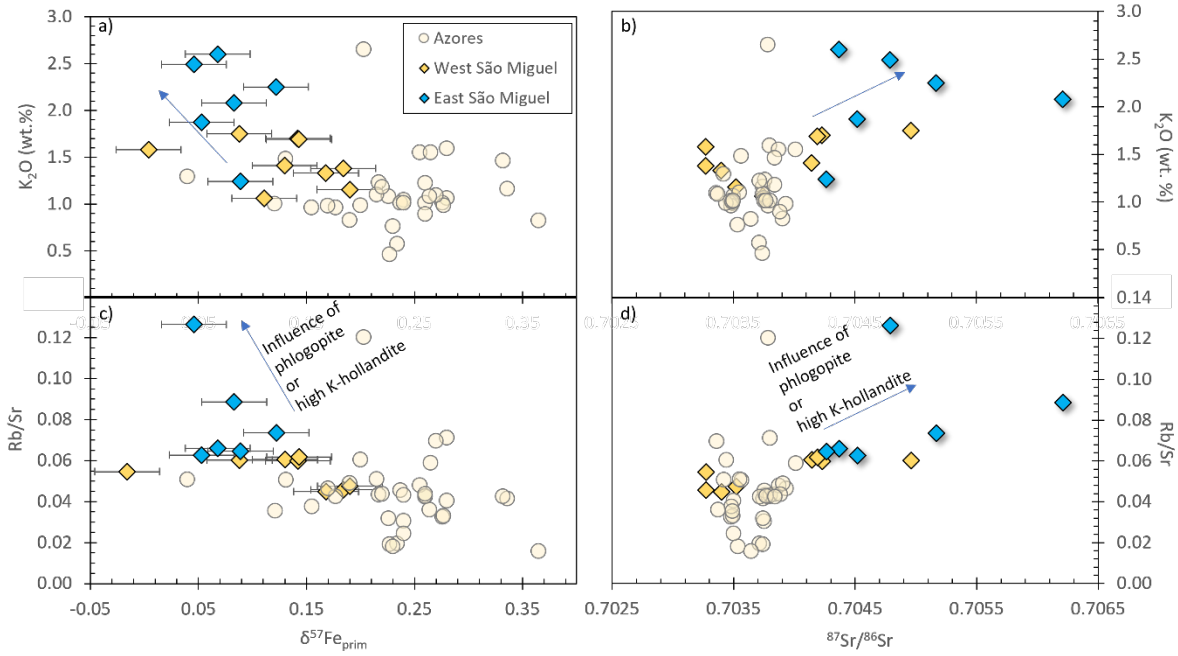


Figure 6. a) $\delta^{57}Fe_{prim}$ vs K_2O, b) $^{87}Sr/^{86}Sr$ vs K_2O, c) $\delta^{57}Fe_{prim}$ vs Rb/Sr, d) $^{87}Sr/^{86}Sr$ vs Rb/Sr. Increasing K_2O and Rb/Sr indicate the influence of phlogopite or K-rich hollandite. Azores (São Jorge, Pico, Faial, Terceira, João de Castro and Graciosa) from Soderman et al. (2021).

Overall, the sum of observations, including the low melting degree (Beier et al., 2013), indicate that a small volume of a hydrous silicic, K-rich melt could act as a metasomatizing agent at São Miguel, similar to previous suggestions (Widom and Farquhar, 2003). This is further supported by covariations between K_2O and Rb/Sr and radiogenic isotopes (e.g., Fig. 6b, d and Supplementary Data Fig. S4). Considering that small amounts of such metasomatising agent mixes with peridotite, the range in $\delta^{57}Fe_{prim}$ of +0.05 to +0.12‰ can be achieved, depending on the mixing ratio (e.g., ratios between 99:1 and 80:20) of eastern São Miguel's lavas. Whilst the mantle material sourcing São Miguel points towards a metasomatic agent rich in K, it remains unclear how a spatially defined West-East trend can be created by such a source with eastern São Miguel being more effected by this source than western São Miguel lavas.

5.4 The heavy Fe isotopic signature of western São Miguel – Influence of tectonic setting

Western São Miguel lavas are isotopically too heavy to simply reflect partial mantle melting processes of peridotite, which, following modelling, do not exceed values of $\delta^{57}Fe$

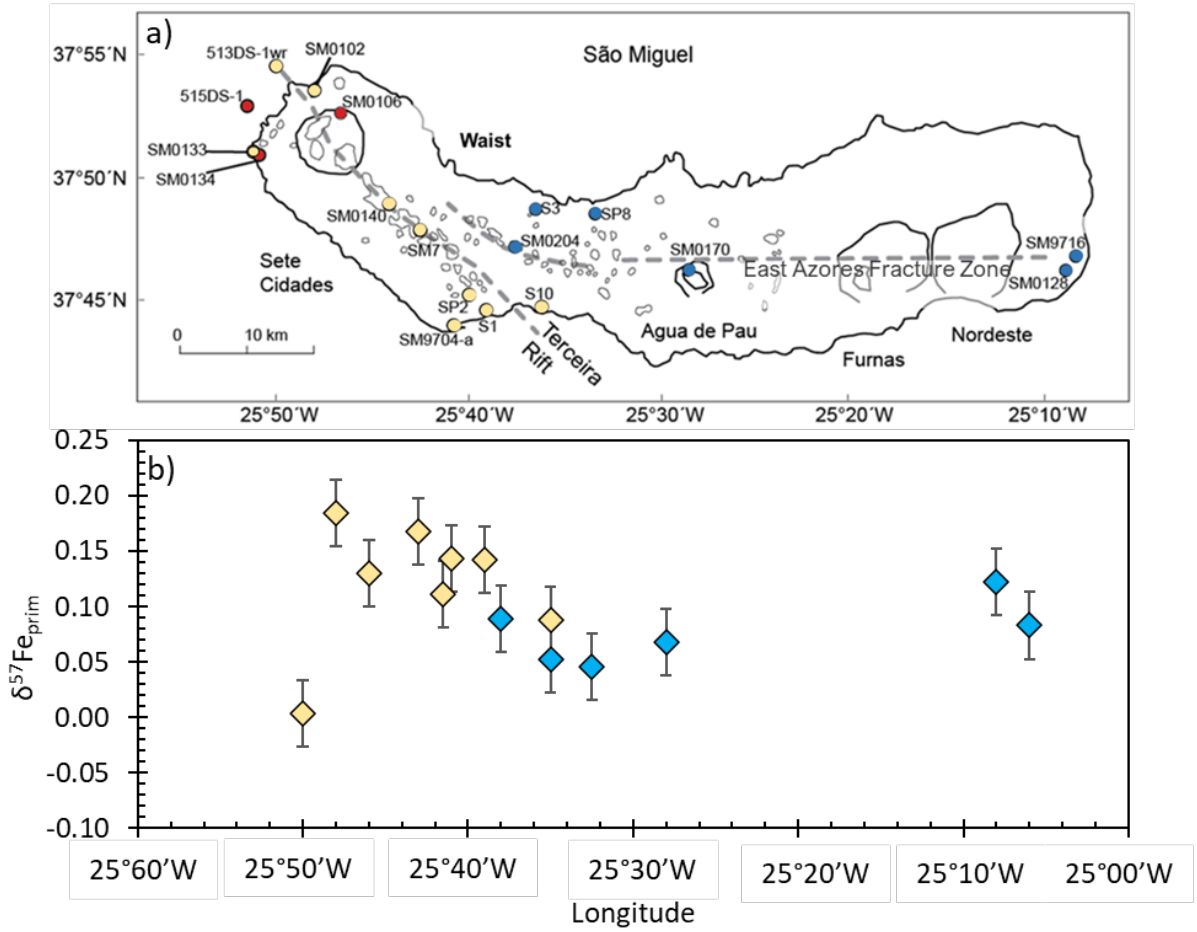
+0.15‰ for a melt fraction < 0.1 (= < 10% partial melting; Foden et al., 2018). The melts also cannot be ascribed to the same metasomatism by the hydrous, silicic melt as mentioned above with a trend towards heavier signatures with a diluted metasomatic component. Both factors point to a second component added to the original metasomatic-derived partial plume melt.

A clue as to why western São Miguel samples are isotopically heavier is their geographic location, which argues for a crustal control on the geochemical signature of these lavas. When projected against the longitude and tectonic structure of São Miguel (Fig. 7), it becomes apparent that all lavas except the outlier sample SM0133 are located along the Terceira Rift, a tectonic structure that runs through the NW part of the island. Melting at a rift setting (Terceira Rift) may thus have a considerable influence on the Fe isotopic composition of western São Miguel's lavas, and in analogue also radiogenic isotopic systematics. More MORB-like radiogenic isotopic systematics in Sr-Nd-Pb isotopes indicate the presence of an upper mantle melting component, which is in line with low, MORB-like $^{3}He/^{4}He$ ratios associated with the Terceira Rift (e.g., Kurz et al., 1990; Madureira et al., 2011).

Compared to OIB, MORB show a homogenous Fe isotopic signature of $\delta^{57}Fe$ +0.15 ± 0.01‰ (Teng et al., 2013; Chen et al., 2019) but can deviate towards heavier Fe isotopes with $\delta^{57}Fe$ ≥ +0.15‰ (Sun et al., 2020). Such heavy Fe isotopic signatures at mid-ocean ridge settings have previously been associated with melting of pyroxenitic veins in the lithosphere (Sun et al., 2020). Ultraslow spreading ridge settings have recently been associated with heavy Fe isotopic compositions (Richter et al., 2021). It has been argued that lavas erupting at such ultraslow spreading ridges preserve the inherited Fe isotopic composition of the source (Richter et al., 2021), which aligns with our samples. Simple addition of a low-degree melt fraction of upper mantle peridotite associated with the Terceira Rift can create a pyroxenite that is not only heavy in Fe isotopes, but also carries MORB-like radiogenic isotopes. The most westerly samples (outlier excluded) in Fig. 7b would therein reflect the most affected lavas through this process of re-melting of such a source, whereas samples towards the east are not affected and only show plume melt components. The mantle source in western São Miguel would thus simply reflect a low-degree MORB melt, either through direct addition or re-melting as pyroxenite, which is superimposed on the original plume-derived melt. Indeed, a contribution of a pyroxenitic/basaltic source to explain heavy Fe isotopic signatures has

been discussed for other Azores locations (São Jorge, Pico, Faial, Terceira, João de Castro and Graciosa; Soderman et al., 2021). Finally, this may also explain the Fe isotopic composition of sample SM0133, which is the lightest in Fe isotopes in the sampled suite. Even though the sample is located in the western part of the island, it is the only sample not located near the rift section and may thus reflect the true nature of the mantle source, i.e., without the rift overprint.

Various aspects of the São Miguel mantle source can be explained with such a hybrid source – one composed of a plume-derived component in the form of a metasomatic section, and one of a low-degree MORB melt. Here it is important to stress that fluids derived from subducted oceanic crust can act as a metasomatic agent, and as such would resemble EM-II type mantle. The origin of this agent remains a matter of debate, whether it originates from the plume itself (through eclogite-facies, resurfacing metasediments) or it is incorporated through lithospheric delamination and subsequent entrainment. Irrespective of this origin, the two-component mantle source can explain the various models proposed for São Miguel. Beier et al. (2007) discuss the possibility of a basaltic melt as a metasomatic agent, but conclude that a basaltic melt of recycled oceanic crust, and not as a metasomatising agent, can explain trace element patterns and radiogenic isotopic signatures of eastern São Miguel's lavas (Fig. 4). Furthermore, a "*basaltic under-plate within an ancient, recycled oceanic lithosphere"* has been suggested by Elliott et al. (2007). For western São Miguel, both scenarios seem plausible, and with a hybrid scenario within a single island, it is clear that no single solution could have been identified previously. Likewise, such a basaltic addition would likely not be enough to overprint oxygen isotopes, which are isotopically lighter in São Miguel lavas (Widom and Farquhar, 2003), noting that this study sampled two lavas from near the Terceira Rift, which are isotopically indistinguishable from the remainder of the island's lavas.



598

599 **Figure 7**. a) Map modified after Beier et al. (2007) showing the sample localities, detailed
600 description in Fig. 1b. b) Longitude vs $\delta^{57}Fe_{prim}$ with western São Miguel samples along the
601 Terceira Rift showing heavier Fe isotopes than eastern São Miguel. An overlap occurs for lavas
602 on the Waist Zone. Agua de Pau and Nordeste show comparable Fe isotopic data to the Waist
603 Zone. One sample of western São Miguel deviates from eastern and western São Miguel by
604 showing a $\delta^{57}Fe_{prim}$ of -0.02‰. This sample lies not on the Terceira Rift.

605 **6. Conclusions**

606 Combined radiogenic Sr-Nd-Pb mantle array proxies with stable Fe isotopic compositions
607 of primary melts from western and eastern São Miguel reveal a complex mantle melting
608 scenario. A correction for igneous differentiation only erases minor effects on Fe isotopic
609 compositions. Consequently, the Fe isotope variability in lavas from São Miguel is not only
610 dependent on differentiation processes occurring during magmatic cooling but also strongly
611 depends on the initial Fe isotopic composition of mantle components. Based on co-variations
612 of stable Fe and radiogenic Sr-Nd-Pb isotopes, the melting regime below São Miguel requires

a scenario in which eastern São Miguel represents a component enriched in radiogenic isotopes and near-chondritic in Fe isotopes. Mass balance calculations revealed that a simple carbonatitic component acting as a metasomatising agent cannot account for this Fe isotopic composition. Rather, the mantle component is suggested to be derived from a source that has experienced mantle metasomatism by a silicic, K-rich melt. Globally, this component is unique among OIB, at least in its pure form. Melting of this component is envisaged here to occur in the asthenospheric mantle within the ascending Azores plumes.

The heavier Fe isotopic signature of western São Miguel's lavas is likely influenced by melting at an ultraslow rift setting. Here, western São Miguel's lavas that are sourced from the same plume region have experienced enrichment in heavier Fe isotopes and incompatible elements by partial re-melting of peridotite that was infused by prior melt addition during rifting, likely in the lithospheric mantle. This additive effect, which is spatially confined to the Terceira Rift on the island, results in Fe isotopes that are too heavy to represent a simple mantle source and mask the true nature of the plume. This process is thus not plume- but plate controlled.

The dichotomy of isotopic systematics within a single volcanic island demonstrates that secondary processes, such as rifts, need to be considered when isotopic ratios are used to trace mantle plume components. For individual ocean island lavas, this highlights the necessity to carefully assess regional tectonic settings before data is placed into a global context. The combination of plume- vs plate-controlled melting adds another complexity to the genesis of ocean island lavas, which can possibly be elucidated with a combination of stable and radiogenic isotopic systematics.

Acknowledgements

We thank Edward Inglis and Geoff Nowell, who helped with the sample preparation and Fe isotope analyses at the Durham University. HMW acknowledges funding from a NERC Consortia Grant ("Deep Volatiles"; NE/M000303/1) and an ERC Consolidator Grants ("HabitablePlanet"; 306655). ON acknowledges funding from the Australian Research Council grant (DP180100852).

642 **References**

643 Beard, B.L. and Johnson, C.M. (2004) Inter-mineral Fe isotope variations in mantle-derived
644 rocks and implications for the Fe geochemical cycle. *Geochimica et cosmochimica acta*
645 **68**, 4727-4743.

646 Béguelin, P., Bizimis, M., Beier, C. and Turner, S. (2017) Rift-plume interaction reveals multiple
647 generations of recycled oceanic crust in Azores lavas. *Geochimica et cosmochimica*
648 *acta* **218**, 132-152.

649 Beier, C., Haase, K.M. and Hansteen, T.H. (2006) Magma Evolution of the Sete Cidades
650 Volcano, São Miguel, Azores. *Journal of Petrology* **47**, 1375-1411.

651 Beier, C., Stracke, A. and Haase, K.M. (2007) The peculiar geochemical signatures of Sao
652 Miguel (Azores) lavas: Metasomatised or recycled mantle sources? *Earth and*
653 *Planetary Science Letters* **259**, 186-199.

654 Beier, C., Haase, K.M., Abouchami, W., Krienitz, M.S. and Hauff, F. (2008) Magma genesis by
655 rifting of oceanic lithosphere above anomalous mantle: Terceira Rift, Azores.
656 *Geochemistry, Geophysics, Geosystems* **9**, Q12013.Beier, C., Haase, K.M. and Turner,
657 S.P. (2012) Conditions of melting beneath the Azores. *Lithos* **144**, 1-11.

658 Beier, C., Mata, J., Stöckhert, F., Mattielli, N., Brandl, P., Madureira, P., Genske, F., Martins, S.,
659 Madeira, J. and Haase, K. (2013) Geochemical evidence for melting of carbonated
660 peridotite on Santa Maria Island, Azores. *Contributions to Mineralogy and Petrology*
661 **165**, 823-841.

662 Beier, C., Haase, K.M. and Brandl, P.A. (2018) Melting and mantle sources in the Azores,
663 Volcanoes of the Azores. Springer, pp. 251-280.

664 Bézos, A. and Humler, E. (2005) The Fe3+/ΣFe ratios of MORB glasses and their implications
665 for mantle melting. *Geochimica et Cosmochimica Acta* **69**, 711-725.

666 Blichert-Toft, J. and Albarede, F. (1998) Hafnium isotope stratigraphy of Mauna Loa and
667 Mauna Kea lavas from the Hawaii Scientific Drilling Project core. *Mineralogical*
668 *Magazine* **62**, 166-167.

669 Booth, B., Croasdale, R. and Walker, G.P.L. (1978) A Quantitative Study of Five Thousand Years
670 of Volcanism on Sao Miguel, Azores. *Philosophical Transactions of the Royal Society of*
671 *London. Series A, Mathematical and Physical Sciences (1934-1990)* **288**, 271-319.

672 Chase, C.G. (1981) Oceanic island Pb: two-stage histories and mantle evolution. *Earth and*
673 *Planetary Science Letters* **52**, 277-284.
674 Chen, S., Niu, Y., Guo, P., Gong, H., Sun, P., Xue, Q., Duan, M. and Wang, X. (2019) Iron isotope
675 fractionation during mid-ocean ridge basalt evolution: Evidence from lavas on the East
676 Pacific Rise at 10°30'N and its implications. *Geochimica et cosmochimica acta* **267**, p
677 227-239.
678 Cheng, T., Nebel, O., Sossi, P.A. and Chen, F. (2014) Refined separation of combined Fe-Hf
679 from rock matrices for isotope analyses using AG-MP-1M and Ln-Spec
680 chromatographic extraction resins. *MethodsX* **1**, 144-150.
681 Craddock, P.R. and Dauphas, N. (2010) Iron Isotopic Compositions of Geological Reference
682 Materials and Chondrites. *Geostandards and Geoanalytical Research* **35**, 101-123.
683 Craddock, P.R., Warren, J.M. and Dauphas, N. (2013) Abyssal peridotites reveal the near-
684 chondritic Fe isotopic composition of the Earth. *Earth and Planetary Science Letters*
685 **365**, 63-76.
686 Dauphas, N., Craddock, P.R., Asimow, P.D., Bennett, V.C., Nutman, A.P. and Ohnenstetter, D.
687 (2009) Iron isotopes may reveal the redox conditions of mantle melting from Archean
688 to Present. *Earth and planetary science letters* **288**, 255-267.
689 Davies, G.R., Cliff, R.A., Norry, M.J. and Gerlach, D.C. (1989) A combined chemical and Pb-Sr-
690 Nd isotope study of the Azores and Cape Verde hot-spots: The geodynamic
691 implications. *Geological Society Special Publication* **42**, 231-255.
692 Du, D.-H., Wang, X.-L., Yang, T., Chen, X., Li, J.-Y. and Li, W. (2017) Origin of heavy Fe isotope
693 compositions in high-silica igneous rocks: A rhyolite perspective. *Geochimica et*
694 *cosmochimica acta* **218**, 58-72.
695 Duncan, A.M., Guest, J.E., Wallenstein, N. and Chester, D.K. (2015) The Older Volcanic
696 Complexes of São Miguel, Azores: Nordeste and Povoação. *Geological Society, London,*
697 *Memoirs* **44**, 147-153.
698 El Korh, A., Luais, B., Deloule, E. and Cividini, D. (2017) Iron isotope fractionation in
699 subduction-related high-pressure metabasites (Ile de Groix, France). *Contributions to*
700 *Mineralogy and Petrology* **172**, 1-19.
701 Elliott, T., Blichert-Toft, J., Heumann, A., Koetsier, G. and Forjaz, V. (2007) The origin of
702 enriched mantle beneath São Miguel, Azores. *Geochimica et Cosmochimica Acta* **71**,
703 219-240.

Fitton, J.G., Saunders, A.D., Kempton, P.D. and Hardarson, B.S. (2003) Does depleted mantle form an intrinsic part of the Iceland plume? *Geochemistry, Geophysics, Geosystems* **4**, 1032.

Foden, J., Sossi, P.A. and Nebel, O. (2018) Controls on the iron isotopic composition of global arc magmas. *Earth and Planetary Science Letters* **494**, 190-201.

Forjaz, V.H. (1986) Ilha de S. Miguel (Acores)—Carta tectónica na escala 1: 50.000. *Doc. Int. CV/INIC* **9**, 86.

Genske, F.S., Beier, C., Haase, K.M., Turner, S.P., Krumm, S. and Brandl, P.A. (2013) Oxygen isotopes in the Azores islands: Crustal assimilation recorded in olivine. *Geology* **41**, 491-494.

Haase, K.M. and Beier, C. (2003) Tectonic control of ocean island basalt sources on São Miguel, Azores? *Geophysical Research Letters* **30**, 1856.

Hart, S.R., Hauri, E., Oschmann, L.A. and Whitehead, J.A. (1992) Mantle Plumes and Entrainment: Isotopic Evidence. *Science* **256**, 517.

Hauri, E.H., Shimizu, N., Dieu, J.J. and Hart, S.R. (1993) Evidence for hotspot-related carbonatite metasomatism in the oceanic upper mantle. *Nature (London)* **365**, 221-227.

Herzberg, C. (2011) Identification of Source Lithology in the Hawaiian and Canary Islands: Implications for Origins. *Journal of Petrology* **52**, 113-146.

Hofmann, A.W. (1997) Mantle geochemistry: the message from oceanic volcanism. *Nature* **385**, 219.

Hofmann, A.W. and White, W.M. (1982) Mantle plumes from ancient oceanic crust. *Earth and planetary science letters* **57**, 421-436.

Hofmann, A.W. and White, W.M. (1983) Ba, Rb and Cs in the Earth's mantle. *Zeitschrift für Naturforschung A* **38**, 256-266.

Hofmann, A.W. (2003) Sampling Mantle Heterogeneity through Oceanic Basalts: Isotopes and Trace Elements, in Treatise on Geochemistry: The Mantle and Core, edited by R. W. Carlson, H.D. Holland, and K.K. Turekian. Elsevier, New York, pp. 61-101.

Hofmann, A.W. and Farnetani, C.G. (2013) Two views of Hawaiian plume structure. *Geochemistry, Geophysics, Geosystems* **14**, 5308-5322.

734 Jackson, M.G., Kurz, M.D., Hart, S.R. and Workman, R.K. (2007) New Samoan lavas from Ofu
735 Island reveal a hemispherically heterogeneous high 3He/ 4He mantle. *Earth and*
736 *Planetary Science Letters* **264**, 360-374.
737 Johnson, C.L., Wijbrans, J.R., Constable, C.G., Gee, J., Staudigel, H., Tauxe, L., Forjaz, V.-H. and
738 Salgueiro, M. (1998) 40Ar/39Ar ages and paleomagnetism of Sao Miguel lavas, Azores.
739 *Earth and Planetary Science Letters* **160**, 637-649.
740 Johnson, C., Bell, K., Beard, B. and Shultis, A. (2010) Iron isotope compositions of carbonatites
741 record melt generation, crystallization, and late-stage volatile-transport processes.
742 *Mineralogy and Petrology* **98**, 91-110.
743 King, S.D. and Adam, C. (2014) Hotspot swells revisited. *Physics of the Earth and Planetary*
744 *Interiors* **235**, 66.
745 Konter, J.G., Pietruszka, A.J., Hanan, B.B., Finlayson, V.A., Craddock, P.R., Jackson, M.G. and
746 Dauphas, N. (2016) Unusual δ56Fe values in Samoan rejuvenated lavas generated in
747 the mantle. *Earth and Planetary Science Letters* **450**, 221-232.
748 Koppers, A.A., Becker, T.W., Jackson, M.G., Konrad, K., Müller, R.D., Romanowicz, B.,
749 Steinberger, B. and Whittaker, J.M. (2021) Mantle plumes and their role in Earth
750 processes. *Nature Reviews Earth & Environment*, 1-20.
751 Kurz, M., Kammer, D., Gulessarian, A. and Moore, R. (1990) Isotopic variations within oceanic
752 islands: He, Sr and Pb isotopes in basalts from São Miguel, Azores. *Eos* **71**, 657.
753 Larrea, P., França, Z., Widom, E. and Lago, M. (2018) Petrology of the Azores Islands,
754 Volcanoes of the Azores. Springer, pp. 197-249.
755 Lassiter, J. and Hauri, E. (1998) Osmium-isotope variations in Hawaiian lavas: evidence for
756 recycled oceanic lithosphere in the Hawaiian plume. *Earth and Planetary Science*
757 *Letters* **164**, 483-496.
758 LaTourrette, T., Hervig, R.L. and Holloway, J.R. (1995) Trace element partitioning between
759 amphibole, phlogopite, and basanite melt. *Earth and Planetary Science Letters* **135**,
760 13-30.
761 Madureira, P., Moreira, M., Nunes, J.C., Lourenço, N., Gautheron, C., Carvalho, M.d.R., Mata,
762 J. and Pinto de Abreu, M. (2011) He and Ne isotopic ratios from the Terceira Rift
763 (Azores): Constraints on the boundary between Eurasia and Nubia mantle sources.
764 *Mineralogical Magazine* **75** (3), 1383.

765 Mattielli, N., Weis, D., Scoates, J.S., Shimizu, N., GreGoire, M., Mennessier, J.P., Cottin, J.Y.
766 and Giret, A. (1999) Evolution of Heterogeneous Lithospheric Mantle in a Plume
767 Environment Beneath the Kerguelen Archipelago. *Journal of petrology* **40**, 1721-1744.

768 McCoy-West, A.J., Fitton, J.G., Pons, M.-L., Inglis, E.C., Williams, H.M., (2018) The Fe and Zn isotope
769 composition of deep mantle source regions: Insights from Baffin Island picrites. *Geochimica*
770 *et Cosmochimica Acta* **238,** 542-562. 10.1016/j.gca.2018.07.021.

771 Métrich, N., Zanon, V., Créon, L., Hildenbrand, A., Moreira, M. and Marques, F.O. (2014) Is the
772 'Azores hotspot'a wetspot? Insights from the geochemistry of fluid and melt inclusions
773 in olivine of Pico basalts. *Journal of Petrology* **55**, 377-393.
774 Moreira, M., Kanzari, A. and Madureira, P. (2012) Helium and neon isotopes in São Miguel
775 island basalts, Azores Archipelago: New constraints on the "low 3He" hotspot origin.
776 *Chemical geology* **322-323**, 91-98.
777 Moreira, M.A., Madureira, P. and Mata, J. (2018) Noble gas constraints on the origin of the
778 Azores hotspot, Volcanoes of the Azores. Springer, pp. 281-299.
779 Nebel, O., Campbell, I.H., Sossi, P.A. and Van Kranendonk, M.J. (2014) Hafnium and iron
780 isotopes in early Archean komatiites record a plume-driven convection cycle in the
781 Hadean Earth. *Earth and Planetary Science Letters* **397**, 111-120.
782 Nebel, O., Sossi, P.A., Bénard, A., Wille, M., Vroon, P.Z. and Arculus, R.J. (2015) Redox-
783 variability and controls in subduction zones from an iron-isotope perspective. *Earth*
784 *and Planetary Science Letters* **432**, 142-151.
785 Nebel, O., Sossi, P.A., Foden, J., Bénard, A., Brandl, P.A., Stammeier, J.A., Lupton, J., Richter,
786 M. and Arculus, R.J. (2018) Iron isotope variability in ocean floor lavas and mantle
787 sources in the Lau back-arc basin. *Geochimica et Cosmochimica Acta* **241**, 150-163.
788 Nebel, O., Sossi, P.A., Bénard, A., Arculus, R.J., Yaxley, G.M., Woodhead, J.D., Rhodri Davies,
789 D. and Ruttor, S. (2019) Reconciling petrological and isotopic mixing mechanisms in
790 the Pitcairn mantle plume using stable Fe isotopes. *Earth and Planetary Science Letters*
791 **521**, 60-67.
792 Palme, H. and O'Neill, H.S.C. (2014) Cosmochemical Estimates of Mantle Composition, in:
793 Carlson, R.W.E. (Ed.), Treatise on Geochemistry. Elsevier B.V., Amsterdam, pp. 1-38.

794 Pietruszka, A.J., Norman, M.D., Garcia, M.O., Marske, J.P. and Burns, D.H. (2013) Chemical
795 heterogeneity in the Hawaiian mantle plume from the alteration and dehydration of
796 recycled oceanic crust. *Earth and Planetary Science Letters* **361**, 298-309.
797 Poitrasson, F., Delpech, G. and GrΓ©goire, M. (2013) On the iron isotope heterogeneity of
798 lithospheric mantle xenoliths: implications for mantle metasomatism, the origin of
799 basalts and the iron isotope composition of the Earth. *Contributions to mineralogy and*
800 *petrology* **165**, 1243-1258.
801 Prytulak, J. and Elliott, T. (2007) TiO2 enrichment in ocean island basalts. *Earth and Planetary*
802 *Science Letters* **263**, 388-403.
803 Prytulak, J., Avanzinelli, R., Koetsier, G., Kreissig, K., Beier, C. and Elliott, T. (2014) Melting
804 versus contamination effects on U-238-Th-230-Ra-226 and U-235-Pa-231 disequilibria
805 in lavas from Sao Miguel, Azores. *Chemical Geology* **381**, 94-109.
806 Richter, M., Nebel, O., Schwindinger, M., Nebel-Jacobsen, Y. and Dick, H.J. (2021) Competing
807 effects of spreading rate, crystal fractionation and source variability on Fe isotope
808 systematics in mid-ocean ridge lavas. *Scientific reports* **11**, 1-15.
809 Roeder, P. and Emslie, R. (1970) Olivine-liquid equilibrium. *Contributions to Mineralogy and*
810 *Petrology* **29**, 275-289.
811 Romer, R.H., Beier, C., Haase, K.M., Eberts, A. and Hübscher, C. (2021) The evolution of central
812 volcanoes in ultraslow rift systems: Constraints from D. João de Castro seamount,
813 Azores. *Tectonics* **40**, e2020TC006663.
814 Rouxel, O., Dobbek, N., Ludden, J. and Fouquet, Y. (2003) Iron isotope fractionation during
815 oceanic crust alteration. *Chemical Geology* **202**, 155-182.
816 Ryan, W.B., Carbotte, S.M., Coplan, J.O., O'Hara, S., Melkonian, A., Arko, R., Weissel, R.A.,
817 Ferrini, V., Goodwillie, A. and Nitsche, F. (2009) Global multi‐resolution topography
818 synthesis. *Geochemistry, Geophysics, Geosystems* **10**.
819 Safonov, O., Butvina, V. and Limanov, E. (2019) Phlogopite-Forming Reactions as Indicators of
820 Metasomatism in the Lithospheric Mantle. *Minerals* **9**, 685.
821 Salters, V.J. and White, W.M. (1998) Hf isotope constraints on mantle evolution. *Chemical*
822 *Geology* **145**, 447-460.
823 Salters, V.J.M. and Stracke, A. (2004) Composition of the depleted mantle. *Geochemistry,*
824 *Geophysics, Geosystems* **5**, Q05B07.

825 Searle, R. (1980) Tectonic pattern of the Azores spreading centre and triple junction. *Earth*
826 *and Planetary Science Letters* **51**, 415-434.Sobolev, A., V. , Hofmann, A., W. and
827 Nikogosian, I., K. (2000) Recycled oceanic crust observed in 'ghost plagioclase' within
828 the source of Mauna Loa lavas. *Nature* **404**, 986.
829 Sobolev, A.V., Hofmann, A.W., Kuzmin, D.V., Yaxley, G.M., Arndt, N.T., Chung, S.L.,
830 Danyushevsky, L.V., Elliott, T., Frey, F.A., Garcia, M.O., Gurenko, A.A., Kamenetsky, V.S.,
831 Kerr, A.C., Krivolutskaya, N.A., Matvienkov, V.V., Nikogosian, I.K., Rocholl, A.,
832 Sigurdsson, I.A., Sushchevskaya, N.M. and Teklay, M. (2007) The Amount of Recycled
833 Crust in Sources of Mantle-Derived Melts. *Science* **316**, 412-417.
834 Soderman, C.R., Matthews, S., Shorttle, O., Jackson, M.G., Ruttor, S., Nebel, O., Turner, S.,
835 Beier, C., Millet, M.-A., Widom, E., Humayun, M. and Williams, H.M. (2021) Heavy
836 δ57Fe in ocean island basalts: a non-unique signature of processes and source
837 lithologies in the mantle. *Geochimica et Cosmochimica Acta* **292**, 309-332.
838 Sossi, P., Foden, J. and Halverson, G. (2012) Redox-controlled iron isotope fractionation during
839 magmatic differentiation: an example from the Red Hill intrusion, S. Tasmania.
840 *Contributions to Mineralogy and Petrology* **164**, 757-772.
841 Sossi, P.A., Halverson, G.P., Nebel, O. and Eggins, S.M. (2015) Combined Separation of Cu, Fe
842 and Zn from Rock Matrices and Improved Analytical Protocols for Stable Isotope
843 Determination. *Geostand. Geoanal. Res.* **39**, 129-149.
844 Sossi, P.A., Nebel, O. and Foden, J. (2016) Iron isotope systematics in planetary reservoirs.
845 *Earth and Planetary Science Letters* **452**, 295-308.
846 Sossi, P.A. and O'Neill, H.S.C. (2017) The effect of bonding environment on iron isotope
847 fractionation between minerals at high temperature. *Geochimica et Cosmochimica*
848 *Acta* **196**, 121-143.
849 Standish, J.J., Dick, H.J., Michael, P.J., Melson, W.G. and O'Hearn, T. (2008) MORB generation
850 beneath the ultraslow spreading Southwest Indian Ridge (9–25 E): Major element
851 chemistry and the importance of process versus source. *Geochemistry, Geophysics,*
852 *Geosystems* **9**, Q05004.
853 Stracke, A., Hofmann, A.W. and Hart, S.R. (2005) FOZO, HIMU, and the rest of the mantle zoo.
854 *Geochemistry, Geophysics, Geosystems* **6**, Q05007.
855 Stracke, A. (2012) Earth's heterogeneous mantle: A product of convection-driven interaction
856 between crust and mantle. *Chemical Geology* **330**, 274-299.

Sun, P., Niu, Y., Guo, P., Duan, M., Chen, S., Gong, H., Wang, X. and Xiao, Y. (2020) Large iron isotope variation in the eastern Pacific mantle as a consequence of ancient low-degree melt metasomatism. *Geochimica et Cosmochimica Acta* **286**, 269-288.

Teng, F.-Z., Dauphas, N. and Helz, R.T. (2008) Iron isotope fractionation during magmatic differentiation in Kilauea Iki lava lake. *Science (New York, N.Y.)* **320**, 1620.

Teng, F.-Z., Dauphas, N., Helz, R.T., Gao, S. and Huang, S. (2011) Diffusion-driven magnesium and iron isotope fractionation in Hawaiian olivine. *Earth and planetary science letters* **308**, 317-324.

Teng, F.-Z., Dauphas, N., Huang, S. and Marty, B. (2013) Iron isotopic systematics of oceanic basalts. *Geochimica et Cosmochimica Acta* **107**, 12-26.

Turner, S., Hawkesworth, C., Rogers, N. and King, P. (1997) U-Th isotope disequilibria and ocean island basalt generation in the Azores. *Chem. Geol.* **139**, 145-164.

Turner, S., Tonarini, S., Bindeman, I., Leeman, W., P. and Schaefer, B., F. (2007) Boron and oxygen isotope evidence for recycling of subducted components over the past 2.5Gyr. *Nature* **447**, 702.

Vogt, P.R. and Jung, W.Y. (2004) The Terceira Rift as hyper-slow, hotspot-dominated oblique spreading axis: A comparison with other slow-spreading plate boundaries. *Earth and Planetary Science Letters* **218**, 77-90.

Wang, X.-J., Chen, L.-H., Hofmann, A.W., Hanyu, T., Kawabata, H., Zhong, Y., Xie, L.-W., Shi, J.-H., Miyazaki, T., Hirahara, Y., Takahashi, T., Senda, R., Chang, Q., Vaglarov, B.S. and Kimura, J.-I. (2018) Recycled ancient ghost carbonate in the Pitcairn mantle plume. *Proceedings of the National Academy of Sciences of the United States* **115**, 8682.

Weis, D., Garcia, M., O., Rhodes, J.M., Jellinek, M. and Scoates, J., S. (2011) Role of the deep mantle in generating the compositional asymmetry of the Hawaiian mantle plume. *Nature Geoscience* **4**, 831.

Wendt, I. and Carl, C. (1991) The statistical distribution of the mean squared weighted deviation. *Chemical Geology: Isotope Geoscience Section* **86**, 275-285.

Weyer, S. and Ionov, D.A. (2007) Partial melting and melt percolation in the mantle: The message from Fe isotopes. *Earth and Planetary Science Letters* **259**, 119-133.

White, W.M., Tapia, M.D. and Schilling, J.-G. (1979) The petrology and geochemistry of the Azores Islands. *Contributions to Mineralogy and Petrology* **69**, 201-213.

White, W.M. (2015) Isotopes, DUPAL, LLSVPs, and Anekantavada. *Chemical Geology* **419**, 10-28.

Widom, E., Carlson, R.W., Gill, J.B. and Schmincke, H.U. (1997) Th–Sr–Nd–Pb isotope and trace element evidence for the origin of the São Miguel, Azores, enriched mantle source. *Chemical geology* **140**, 49-68.

Widom, E. and Farquhar, J. (2003) Oxygen isotope signatures in olivines from São Miguel (Azores) basalts: implications for crustal and mantle processes. *Chemical geology* **193**, 237-255.

Williams, H.M., Peslier, A.H., McCammon, C., Halliday, A.N., Levasseur, S., Teutsch, N. and Burg, J.P. (2005) Systematic iron isotope variations in mantle rocks and minerals: The effects of partial melting and oxygen fugacity. *Earth and Planetary Science Letters* **235**, 435-452.

Williams, H.M., Nielsen, S.G., Renac, C., Griffin, W.L., O'Reilly, S.Y., McCammon, C.A., Pearson, N., Viljoen, F., Alt, J.C. and Halliday, A.N. (2009) Fractionation of oxygen and iron isotopes by partial melting processes: Implications for the interpretation of stable isotope signatures in mafic rocks. *Earth and Planetary Science Letters* **283**, 156-166.

Williams, H.M. and Bizimis, M. (2014) Iron isotope tracing of mantle heterogeneity within the source regions of oceanic basalts. *Earth and Planetary Science Letters* **404**, 396-407.

Woodland, A.B. and Koch, M. (2003) Variation in oxygen fugacity with depth in the upper mantle beneath the Kaapvaal craton, Southern Africa. *Earth and planetary science letters* **214**, 295-310.

Ye, H., Wu, C., Brzozowski, M.J., yang, T., Zha, X., Gao, B., Li, W. (2020): Calibrating equilibrium Fe isotope fractionation factors between magnetite, garnet, amphibole and biotite, Geochimica et Cosmochimica Acta, Vol., 2071, p., 78-95

Zhao, X., Zhang, H., Zhu, X., Tang, S. and Yan, B. (2012) Iron isotope evidence for multistage melt–peridotite interactions in the lithospheric mantle of eastern China. *Chemical geology* **292**, 127-139.

Zindler, A. and Hart, S. (1986) Chemical geodynamics. *Annual Review of Earth and Planetary Sciences* **14**, 493-571.